



HAL
open science

Chemical Synthesis of TFF3 Reveals Novel Mechanistic Insights and a Gut-Stable Metabolite

Nayara Braga Emidio, Rajeshwari Meli, Hue Tran, Hayeon Baik, Séverine Morisset-Lopez, Alysha Elliott, Mark Blaskovich, Sabrina Spiller, Annette Beck-Sickinger, Christina Schroeder, et al.

► **To cite this version:**

Nayara Braga Emidio, Rajeshwari Meli, Hue Tran, Hayeon Baik, Séverine Morisset-Lopez, et al.. Chemical Synthesis of TFF3 Reveals Novel Mechanistic Insights and a Gut-Stable Metabolite. *Journal of Medicinal Chemistry*, 2021, 64 (13), pp.9484-9495. 10.1021/acs.jmedchem.1c00767 . hal-03335490

HAL Id: hal-03335490

<https://hal.science/hal-03335490v1>

Submitted on 21 Nov 2021

HAL is a multi-disciplinary open access archive for the deposit and dissemination of scientific research documents, whether they are published or not. The documents may come from teaching and research institutions in France or abroad, or from public or private research centers.

L'archive ouverte pluridisciplinaire **HAL**, est destinée au dépôt et à la diffusion de documents scientifiques de niveau recherche, publiés ou non, émanant des établissements d'enseignement et de recherche français ou étrangers, des laboratoires publics ou privés.

1 Chemical Synthesis of TFF3 Reveals Novel Mechanistic Insights and 2 a Gut-Stable Metabolite

3 Nayara Braga Emidio, Rajeshwari Meli, Hue N. T. Tran, Hayeon Baik, Séverine Morisset-Lopez,
4 Alysha G. Elliott, Mark A. T. Blaskovich, Sabrina Spiller, Annette G. Beck-Sickinger,
5 Christina I. Schroeder, and Markus Muttenthaler*



Cite This: <https://doi.org/10.1021/acs.jmedchem.1c00767>



Read Online

ACCESS |



Metrics & More

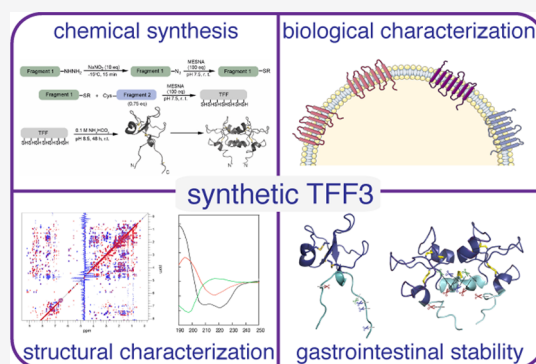


Article Recommendations



Supporting Information

6 **ABSTRACT:** TFF3 regulates essential gastro- and neuroprotective
7 functions, but its molecular mode of action remains poorly understood.
8 Synthetic intractability and lack of reliable bioassays and validated receptors
9 are bottlenecks for mechanistic and structure–activity relationship studies.
10 Here, we report the chemical synthesis of TFF3 and its homodimer *via* native
11 chemical ligation followed by oxidative folding. Correct folding was
12 confirmed by NMR and circular dichroism, and TFF3 and its homodimer
13 were not cytotoxic or hemolytic. TFF3, its homodimer, and the trefoil
14 domain (TFF3₁₀₋₅₀) were susceptible to gastrointestinal degradation,
15 revealing a gut-stable metabolite (TFF3₇₋₅₄; $t_{1/2}$ > 24 h) that retained its
16 trefoil structure and antiapoptotic bioactivity. We tried to validate the
17 putative TFF3 receptors CXCR4 and LINGO2, but neither TFF3 nor its
18 homodimer displayed any activity up to 10 μ M. The discovery of a gut-stable
19 bioactive metabolite and reliable synthetic accessibility to TFF3 and its analogues are cornerstones for future molecular probe
20 development and structure–activity relationship studies.



21 ■ INTRODUCTION

22 The trefoil factor family (TFF) comprises three disulfide-rich
23 peptides (TFF1, TFF2, TFF3) that are abundantly secreted in
24 the gastrointestinal tract where they regulate gut homeostasis
25 by promoting gut protection and repair.^{1–5} They are also
26 expressed in mucosal tissues outside the gut, including in the
27 respiratory tract, urinary tract, uterus, eyes, and salivary glands,
28 where they have similar mucosal repair and protective
29 functions. TFF peptides have also been observed in human
30 breast milk and the brain,^{1,6,7} and have been implicated in
31 cancer development.^{1,8,9}

32 TFF3 is highly expressed in the gastrointestinal mucosa,
33 particularly in the small intestine and colon, where it protects,
34 maintains, and repairs the gastrointestinal tract.^{4,10–17} In the
35 central nervous system (CNS), TFF3 is secreted by neurons
36 and regulates physiological effects such as neuroinflammation¹⁸
37 and behavioral processes including learning and memory¹⁹ and
38 depression.^{20,21} The anti-inflammatory effects of TFF3 on
39 microglia cells (reduced expression and secretion of pro-
40 inflammatory cytokines) and its capacity to mitigate ischemic
41 cerebral injuries by reducing cell death *via* suppression of
42 caspase-3 activity further support TFF3's neuroprotective role
43 in the CNS.^{18,22}

44 TFF3 derives from a 94-residue long precursor protein that
45 comprises a 35-residue-long signal peptide followed by the 59-
46 residue-long TFF3 sequence.²³ The mature secreted and

folded TFF3 peptide (TFF3₁₋₅₉) contains a highly conserved
47 trefoil domain (TFF3₁₀₋₅₀) that also defines the other members
48 of the TFF.^{3,24} The trefoil domain contains six conserved
49 cysteine residues (CX₉₋₁₀CX₉CX₄CCX₁₀C motif) forming
50 three intrachain disulfide bonds in the configuration Cys^{I-V},
51 Cys^{II-IV}, and Cys^{III-VI}.^{3,24} This disulfide bond arrangement
52 creates a compact three-loop structure resembling a trefoil
53 shape, which is considered to be metabolically stable based on
54 TFF3's functional role in the gastrointestinal tract.^{3,24,25} Its
55 gastrointestinal stability has, however, not been systematically
56 investigated, and some reports indicate that TFF3 might not be
57 that stable.^{26–28}

58 TFF3 also has an additional C-terminal cysteine residue
59 (Cys^{VII}) located outside the trefoil domain, which enables the
60 formation of covalent homo- or heterodimers (e.g., with the
61 mucus-associated Fc fragment of IgG Fc binding protein,
62 FCGBP).^{29,30} TFF3-FCGBP's function remains unknown, but
63 it is hypothesized to act as a TFF3 reservoir.²⁹ Although the
64 TFF3 homodimer is only present in relatively small
65

Received: April 28, 2021

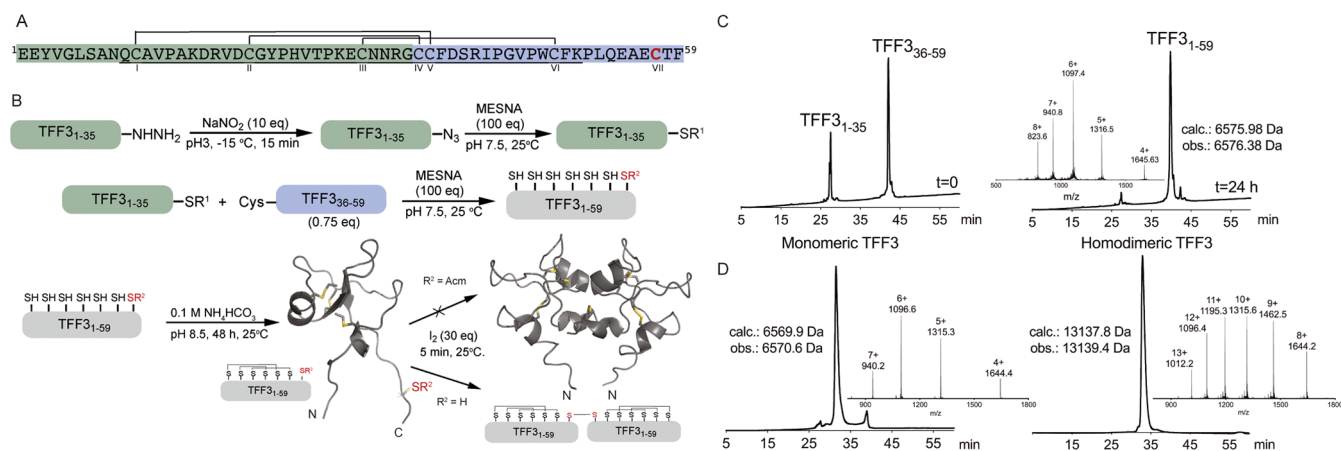


Figure 1. Synthesis of TFF3 and its homodimer. (A) TFF3 sequence and disulfide bond connectivity. Sequence highlighted in green and blue represents the N- and C-terminal fragments used for native chemical ligation, respectively, with Cys⁵⁷ (red) used for dimerization. The trefoil domain is underlined. (B) Synthetic strategy used to produce TFF3 and its homodimer. Highlighted in gray is full-length TFF3. (C) Ligation reaction at time 0 h (left) and 24 h (right). (D) Analytical RP-HPLC chromatogram and MS of folded TFF3 monomer (left) and homodimer (right). TFF3 monomer displays a two-peak RP-HPLC profile due to its conformational complexity (see also Figure S3). TFF3 PDB: 1E9T; TFF3 homodimer PDB: 1PE3.

66 quantities,²⁹ it is more potent than its monomeric counterpart
67 in promoting cell motility.^{31,32} Additionally, only the
68 homodimer but not the monomer displays protective effects
69 when luminally administered in an experimental model of
70 colitis.³²

71 TFF3 can induce several biological effects (i.e., antiapopto-
72 tic,^{33,34} cell migration,^{35–37} and anti-inflammatory effects³⁸),
73 but its mode of action and target receptors have not been fully
74 elucidated nor validated.³⁰ TFF3 was recently described as a
75 natural ligand of the leucine-rich repeat receptor and nogo-
76 interacting protein 2 (LINGO2),³⁸ with TFF3-LINGO2
77 interaction mediating intestinal wound healing and immunity
78 through enhanced epidermal growth factor receptor (EGFR)
79 signaling.³⁸ Another putative receptor is the chemokine
80 receptor type 4 (CXCR4), through which TFF3 might
81 mediate cell migration *via* an ERK1/2-independent signaling
82 pathway.³⁹

83 TFF3 is considered a promising therapeutic lead, especially
84 for disorders requiring epithelial protection, repair, or
85 restitution, such as inflammatory bowel diseases (IBD) and
86 nonsteroidal anti-inflammatory drug-induced gastritis.³⁰ Its
87 therapeutic potential is supported by promising preclinical
88 ^{11,40–42} and clinical studies.^{30,43,44} TFF3 is currently
89 obtained either through recombinant production in *Escherichia*
90 *coli*, *Saccharomyces cerevisiae*, or human embryonic kidney 293
91 (HEK-293) cells,^{45–47} or through purification from milk⁴⁸ or
92 meconium.⁴⁹ These approaches are however not ideal for drug
93 target discovery, where advanced probe development is
94 required, nor for drug development efforts where the
95 incorporation of unnatural amino acids, reporter tags, or
96 conjugation handles at specific positions is often required.
97 Chemical synthesis would allow for such regiospecific control
98 and incorporation of unnatural amino acids, thereby
99 considerably facilitating mechanistic studies and therapeutic
100 development. We thus set out to establish a synthetic strategy
101 to produce TFF3 and its homodimer reliably and in sufficient
102 quantities to deliver new insights into their pharmacology,
103 toxicity, and metabolic stability.

RESULTS

Chemical Synthesis of TFF3, TFF3(C⁵⁷Acm), and TFF3

104
105
106
107
108
109
110
111
112
113
114
115
116
117
118
119
120
121
122
123
124
125
126
127
128
129
130
131
132
133
134
135
136
137
138
139
140
141
142
143
144
145
146
147
148
149
150
151
152
153
154
155
156
157
158
159
160
161
162
163
164
165
166
167
168
169
170
171
172
173
174
175
176
177
178
179
180
181
182
183
184
185
186
187
188
189
190
191
192
193
194
195
196
197
198
199
200
201
202
203
204
205
206
207
208
209
210
211
212
213
214
215
216
217
218
219
220
221
222
223
224
225
226
227
228
229
230
231
232
233
234
235
236
237
238
239
240
241
242
243
244
245
246
247
248
249
250
251
252
253
254
255
256
257
258
259
260
261
262
263
264
265
266
267
268
269
270
271
272
273
274
275
276
277
278
279
280
281
282
283
284
285
286
287
288
289
290
291
292
293
294
295
296
297
298
299
300
301
302
303
304
305
306
307
308
309
310
311
312
313
314
315
316
317
318
319
320
321
322
323
324
325
326
327
328
329
330
331
332
333
334
335
336
337
338
339
340
341
342
343
344
345
346
347
348
349
350
351
352
353
354
355
356
357
358
359
360
361
362
363
364
365
366
367
368
369
370
371
372
373
374
375
376
377
378
379
380
381
382
383
384
385
386
387
388
389
390
391
392
393
394
395
396
397
398
399
400
401
402
403
404
405
406
407
408
409
410
411
412
413
414
415
416
417
418
419
420
421
422
423
424
425
426
427
428
429
430
431
432
433
434
435
436
437
438
439
440
441
442
443
444
445
446
447
448
449
450
451
452
453
454
455
456
457
458
459
460
461
462
463
464
465
466
467
468
469
470
471
472
473
474
475
476
477
478
479
480
481
482
483
484
485
486
487
488
489
490
491
492
493
494
495
496
497
498
499
500
501
502
503
504
505
506
507
508
509
510
511
512
513
514
515
516
517
518
519
520
521
522
523
524
525
526
527
528
529
530
531
532
533
534
535
536
537
538
539
540
541
542
543
544
545
546
547
548
549
550
551
552
553
554
555
556
557
558
559
560
561
562
563
564
565
566
567
568
569
570
571
572
573
574
575
576
577
578
579
580
581
582
583
584
585
586
587
588
589
590
591
592
593
594
595
596
597
598
599
600
601
602
603
604
605
606
607
608
609
610
611
612
613
614
615
616
617
618
619
620
621
622
623
624
625
626
627
628
629
630
631
632
633
634
635
636
637
638
639
640
641
642
643
644
645
646
647
648
649
650
651
652
653
654
655
656
657
658
659
660
661
662
663
664
665
666
667
668
669
670
671
672
673
674
675
676
677
678
679
680
681
682
683
684
685
686
687
688
689
690
691
692
693
694
695
696
697
698
699
700
701
702
703
704
705
706
707
708
709
710
711
712
713
714
715
716
717
718
719
720
721
722
723
724
725
726
727
728
729
730
731
732
733
734
735
736
737
738
739
740
741
742
743
744
745
746
747
748
749
750
751
752
753
754
755
756
757
758
759
760
761
762
763
764
765
766
767
768
769
770
771
772
773
774
775
776
777
778
779
780
781
782
783
784
785
786
787
788
789
790
791
792
793
794
795
796
797
798
799
800
801
802
803
804
805
806
807
808
809
810
811
812
813
814
815
816
817
818
819
820
821
822
823
824
825
826
827
828
829
830
831
832
833
834
835
836
837
838
839
840
841
842
843
844
845
846
847
848
849
850
851
852
853
854
855
856
857
858
859
860
861
862
863
864
865
866
867
868
869
870
871
872
873
874
875
876
877
878
879
880
881
882
883
884
885
886
887
888
889
890
891
892
893
894
895
896
897
898
899
900
901
902
903
904
905
906
907
908
909
910
911
912
913
914
915
916
917
918
919
920
921
922
923
924
925
926
927
928
929
930
931
932
933
934
935
936
937
938
939
940
941
942
943
944
945
946
947
948
949
950
951
952
953
954
955
956
957
958
959
960
961
962
963
964
965
966
967
968
969
970
971
972
973
974
975
976
977
978
979
980
981
982
983
984
985
986
987
988
989
990
991
992
993
994
995
996
997
998
999
1000

After oxidative folding (0.1 M ammonium bicarbonate, pH
8.5, 48 h; Figure S1), we purified TFF3 on a C₅-RP-HPLC
column (Figure 1D, left). The TFF3 homodimer was produced
via the formation of an intermolecular disulfide bond of
unprotected Cys^{VII} (residue 57) through treatment with iodine
(2 min) followed by C₅-RP-HPLC purification (Figure 1D,
right; 60% yield). Since dimerization of TFF3 with the
unprotected Cys^{VII} residue was observed in aqueous solvents at
pH > 7, we also synthesized a TFF3 analogue with Cys^{VII}
protected with an acetamidomethyl (Acm) group (TFF3-
(C⁵⁷Acm)) to prevent dimerization and to ensure clear
functional distinction between monomeric and homodimeric
TFF3 in further studies (Figure S1).

Folded TFF3, whether with Cys^{VII} protected or not, displayed a two-peak profile on analytical HPLC, with each peak having the correct mass (Figures 1D and S2). When these peaks were independently collected and reinjected, the same

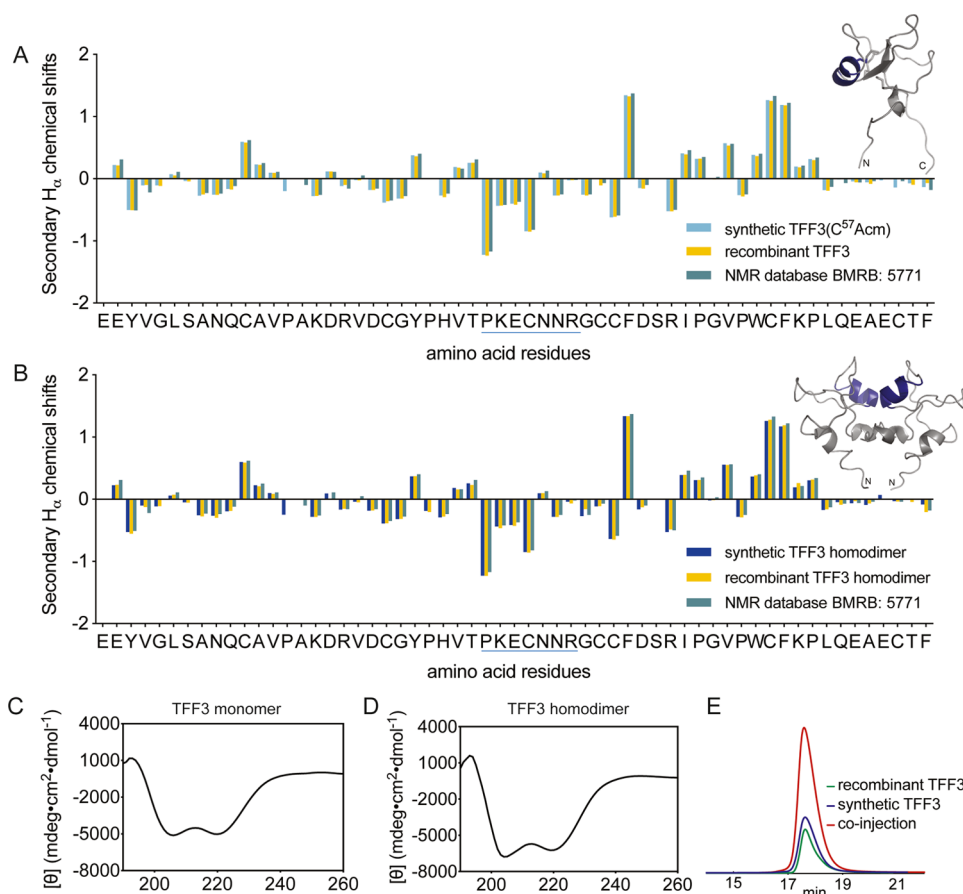


Figure 2. Comparison of secondary H_{α} chemical shifts of (A) TFF3($C^{57}Acm$) and (B) TFF3 homodimer produced by chemical synthesis with recombinant homologues and reported values from the Biological Magnetic Resonance Data Bank (BMRB: 5771). Secondary H_{α} chemical shifts were determined by subtracting the shifts observed in random coil peptides from the shifts determined from the two-dimensional (2D) NMR analysis.⁵⁷ An α -helical region is highlighted in blue in the sequence and NMR structure. CD spectra of synthetic (C) TFF3($C^{57}Acm$) and (D) TFF3 homodimer. (E) Co-elution of synthetic and recombinant TFF3 homodimer (1:2 ratio) on a C_3 -RP-HPLC (1% gradient).

144 two-peak profile was observed (Figure S3), confirming that
 145 both peaks belong to TFF3. This is consistent with the
 146 conformational complexity of TFF3⁴⁵ and an effect commonly
 147 observed with similarly complex peptides and proteins,
 148 including TFF1.^{51–55}

149 **Synthetic TFF3 and TFF3 Homodimer Have the**
 150 **Correct Fold.** We characterized folded TFF3 and TFF3
 151 homodimer by nuclear magnetic resonance (NMR) and
 152 circular dichroism (CD) experiments and compared them
 153 with the structures of recombinant TFF3 and TFF3
 154 homodimer.^{24,56} The H_{α} chemical shifts of TFF3($C^{57}Acm$)
 155 and TFF3 homodimer were assigned using total correlated
 156 spectroscopy (TOCSY) and nuclear Overhauser effect spec-
 157 troscopy (NOESY). Secondary chemical shifts were deter-
 158 mined by subtracting random coil shifts from the H_{α} chemical
 159 shifts.⁵⁷ Comparison of the secondary chemical shift of
 160 synthetic and recombinantly expressed TFF3 (Figure 2A), as
 161 well as those of the corresponding homodimers (Figure 2B),
 162 confirmed the correct fold.^{24,56} CD analysis of synthetic TFF3
 163 indicated the presence of an α -helical structure characterized
 164 by negative bands at 222 and 208 nm and a positive band at
 165 193 nm (Figure 2C,D). This aligned well with the structural
 166 information obtained from recombinant TFF3 provided by Dr.
 167 Lars Thim (Novo Nordisk A/S)⁴⁵ that has a well-defined α -
 168 helix in loop 2. A co-elution study of synthetic and

recombinant TFF3 homodimer further confirmed the NMR 169
 and CD results (Figure 2E). 170

TFF3 and TFF3 Homodimer Reduce Apoptosis of 171
Neuroblastoma Cells. The antiapoptotic activity of TFF3 172
 was reported in cerebral ischemia.²² We therefore evaluated 173
 the capacity of TFF3 and its homodimer to reduce etoposide- 174
 induced cell death, by inhibiting caspase-3/7, in a neuro- 175
 blastoma cell line (SH-SY5Y). TFF3 and its homodimer (10 176
 μ M) induced a statistically significant ($p < 0.05$) reduction in 177
 cell death (Figure 3A). 178

TFF3 and TFF3 Homodimer Are Not Cytotoxic or 179
Hemolytic. Considering the therapeutic potential of TFF3, it 180
 was important to determine any cytotoxic and hemolytic 181
 effects early on to avoid problems in later stages of drug 182
 development. We therefore assessed cytotoxicity on HEK-293 183
 cells and hemolytic effects in human erythrocytes. We treated 184
 the cells with TFF3($C^{57}Acm$) and TFF3 homodimer and used 185
 resazurin, a blue dye that produces strong fluorescence when 186
 reduced by living cells, as the readout of the number of viable 187
 cells.⁶⁰ In the hemolytic assay, we evaluated hemoglobin 188
 release, an indicator of erythrocyte lysis, upon exposure to the 189
 peptides. Neither TFF3($C^{57}Acm$) nor TFF3 homodimer 190
 displayed any cytotoxic or hemolytic effects at the concentra- 191
 tions of up to $\sim 25 \mu$ M (Figure 3B,C). 192

TFF3 and TFF3 Homodimer Do Not Activate CXCR4 193
in COS-7 Cells Overexpressing the Receptor. CXCR4 is a 194

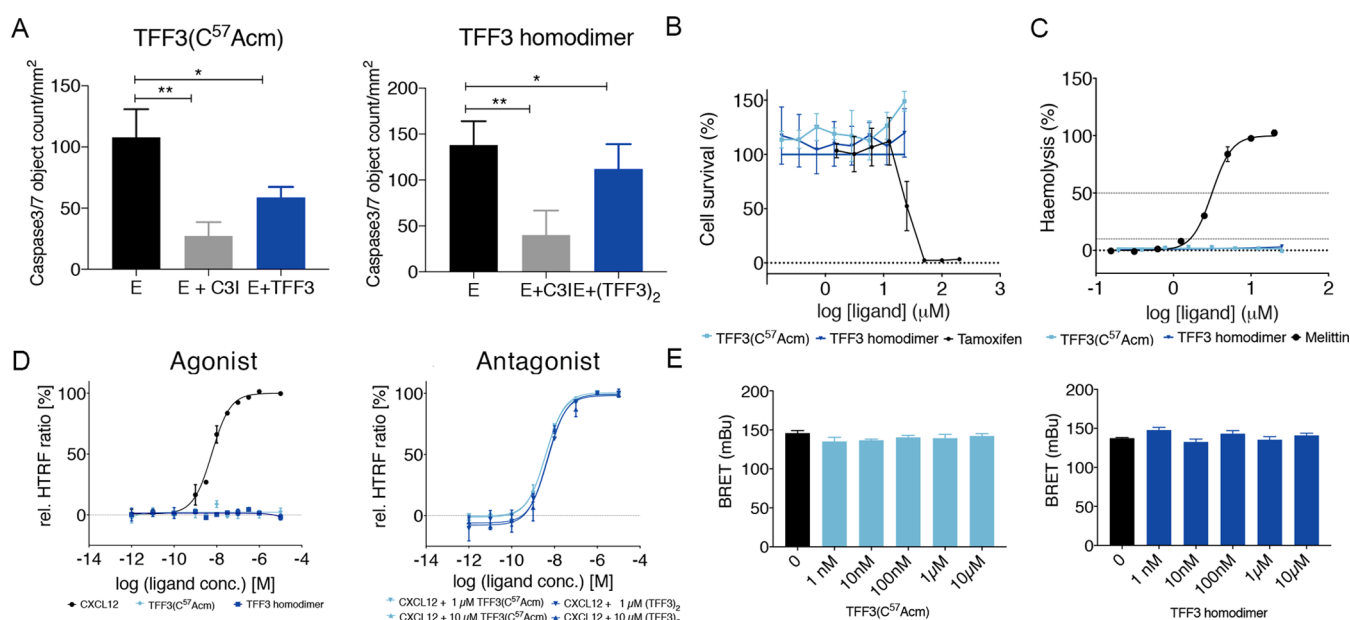


Figure 3. Biological characterization of TFF3(C⁵⁷Acm) and TFF3 homodimer. (A) Cell death was induced with etoposide (10 μ M), and cells were treated with 10 μ M of TFF3. Etoposide and TFF3 were added at the same time. Caspase-3/7 activity was measured after 6 h. The results are expressed (mean \pm standard error of the mean (SEM)) of $n \geq 3$ independent experiments as the number of green fluorescent caspase-3/7 active objects generated by caspase-3/7 reagent added in media. Z-DEVD-FMK (50 μ M; caspase-3 inhibitor) was used as the positive control. E: etoposide, E + C3I: etoposide + caspase-3 inhibitor. One-way analysis of variance (ANOVA) followed by Dunnett correction was performed to assess differences between treated cells and etoposide only. * $p < 0.05$, ** $p < 0.01$. (B) TFF3 effect on the viability of HEK-293 cells after 20 h. Tamoxifen was used as a positive control for cell growth inhibition. Data are representative of two independent experiments shown as mean \pm SEM. (C) Hemolytic activity of TFF3 after 1 h on erythrocytes. Melittin was used as a positive hemolytic control. Data are representative of two independent experiments shown as mean \pm SEM. (D) Effect on CXCR4. Agonistic or antagonistic effects were assessed by the IP1 accumulation assay obtained through homogeneous time-resolved fluorescence (HTRF). CXCL12 was added for antagonistic studies after a 5 min preincubation of TFF3(C⁵⁷Acm) or homodimer. For agonistic evaluation, all compounds were used individually for stimulation in the given concentration range.⁵⁸ Neither TFF3(C⁵⁷Acm) nor TFF3 homodimer were able to activate or inhibit the signal transduction of CXCR4 at concentrations up to 10 μ M, indicating that these peptides are neither agonists nor antagonists at this receptor. The results are expressed as mean \pm SEM of $n \geq 2$ independent experiments. (E) Effect on LINGO2. HEK-293 coexpressing LINGO2-YFP and LINGO2-Rluc were stimulated with increasing amounts of TFF3(C⁵⁷Acm) and TFF3 homodimer (1 nM–10 μ M), but no significant increase in the bioluminescence resonance energy transfer (BRET) signal was observed. No ligand able to alter LINGO2 dimerization is known; therefore, no positive control could be used.⁵⁹ Results are expressed as mean \pm SEM for $n = 4$. One-way ANOVA followed by Dunnett correction was performed to assess differences between treated and nontreated cells.

195 member of the G protein-coupled receptor (GPCR) family⁵⁸
 196 and proposed as a target receptor for TFF3 to mediate wound
 197 healing.^{30,39} We therefore pharmacologically characterized
 198 TFF3(C⁵⁷Acm) and TFF3 homodimer at CXCR4. We used
 199 a chimeric $G\alpha_{iq}$ protein to switch the pathway to the $G\alpha_q$
 200 signaling, which leads to the activation of the phospholipase
 201 and allows measurement of CXCR4 activation through the
 202 production of inositol 1 phosphate (IP1).^{61–63} We measured
 203 IP1 accumulation upon stimulation with TFF3 and TFF3
 204 homodimer in fibroblast-like COS-7 cells transiently trans-
 205 fected with CXCR4.⁵⁸ This is a competitive immunoassay,
 206 based on the HTRF technology, where native IP1 produced by
 207 cells compete with labeled IP1 (acceptor) for binding to anti-
 208 IP1-cryptate (donor). The specific signal (i.e., Förster
 209 resonance energy transfer, FRET) is inversely proportional to
 210 the concentration of IP1 in the sample. The calculation of the
 211 fluorescence ratio eliminates possible medium interferences.⁶⁴
 212 TFF3(C⁵⁷Acm) and TFF3 homodimer were tested alone or
 213 in combination with C-X-C motif chemokine 12 (CXCL12),
 214 the natural CXCR4 ligand,⁵⁸ to assess TFF3's potential to act
 215 as a CXCR4 agonist or antagonist. Neither TFF3(C⁵⁷Acm)
 216 nor TFF3 homodimer activated CXCR4 at concentrations up
 217 to 10 μ M in contrast to the positive control CXCL12 (EC₅₀
 218 5.9 nM) (Figure 3D). The EC₅₀ of CXCL12 was also not

219 affected by TFF3 or TFF3 homodimer (up to 10 μ M), 219
 220 suggesting that these peptides are also not antagonists (Figure 220
 221 3D). 221

TFF3 and TFF3 Homodimer Do Not Activate LINGO2 222
in BRET Assay. LINGO2 has also been put forward as a 223
 224 potential TFF3 receptor.³⁸ We thus evaluated whether 224
 225 TFF3(C⁵⁷Acm) or TFF3 homodimer could disturb LINGO2 225
 226 dimerization *via* a bioluminescence resonance energy transfer 226
 227 (BRET) assay. This method allows the study of protein 227
 228 interactions using energy transfer between a light-emitting 228
 229 enzyme and a fluorescent acceptor protein.⁶⁵ LINGO2 fused 229
 230 with *Renilla* luciferase (Rluc; protein donor) or yellow 230
 231 fluorescent protein (YFP; protein acceptor) were co-expressed 231
 232 in HEK-293 cells and BRET signal detected after adding the 232
 233 luminescent substrate coelenterazine. We observed a strong 233
 234 BRET signal under basal condition, demonstrating the capacity 234
 235 of LINGO2 to form dimers, as already described.⁵⁹ We then 235
 236 evaluated whether the TFF3 constructs could promote changes 236
 237 of this basal BRET signal by inducing conformational change 237
 238 within the dimers and/or change the dimerization state of 238
 239 LINGO2. However, no statistically significant ($p > 0.05$) 239
 240 modification of BRET signal was observed following 240
 241 stimulation of HEK-293 cells coexpressing LINGO2-YFP 241
 242 and LINGO2-Rluc with TFF3(C⁵⁷Acm) or TFF3 homodimer 242

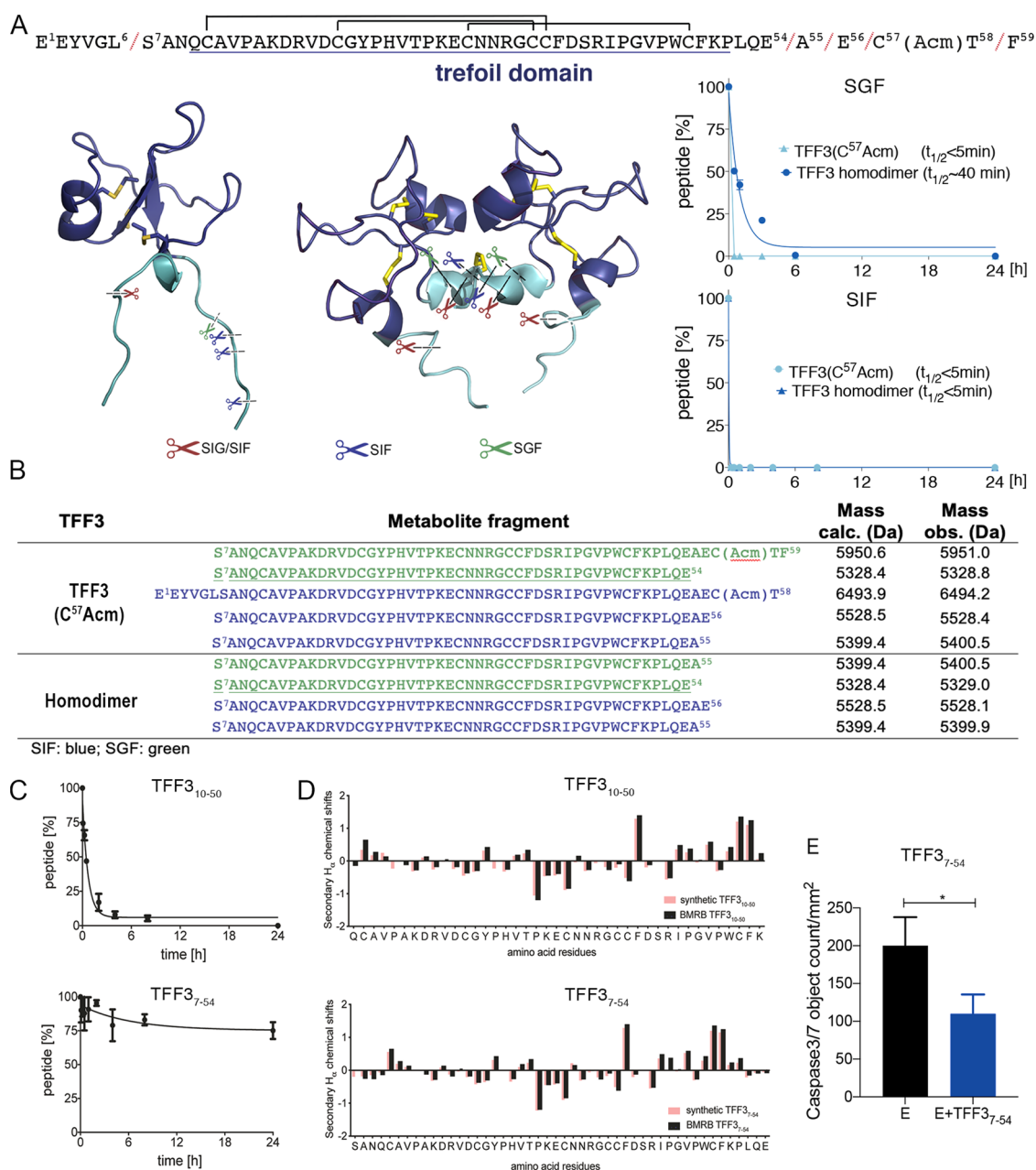


Figure 4. Identification and characterization of a stable and bioactive TFF3 metabolite (TFF3₇₋₅₄). (A) The observed cleavage sites are highlighted in the three-dimensional structure and linear sequence of TFF3. The trefoil domain is underlined and displayed in blue in the sequence and NMR structure. (B) A table listing the observed fragments including their masses. The shortest stable metabolite (TFF3₇₋₅₄) is underlined. (C) Intestinal stability of the trefoil domain TFF3₁₀₋₅₀ and the gut-stable metabolite TFF3₇₋₅₄. (D) Comparison of the secondary H α chemical shifts of TFF3 (BMRB: 5771) and the trefoil domain TFF3₁₀₋₅₀ and TFF3 (BMRB: 5771) and the gut-stable metabolite TFF3₇₋₅₄. Secondary H α chemical shifts were determined by subtracting the shifts observed in random coil peptides from the shifts determined from the 2D NMR analysis.⁵⁷ (E) Antiapoptotic effects of TFF3₇₋₅₄ on SH-SY5Y cells. E: etoposide. Etoposide and TFF3₇₋₅₄ were added at the same time. Caspase-3/7 activity was measured after 6 h. Results are expressed (mean \pm SEM) of $n \geq 3$ independent experiments as the number of green fluorescent caspase-3/7 active objects generated by caspase-3/7 reagent added in media. One-way ANOVA followed by Dunnett correction was performed to assess differences between treated cells and etoposide only. * $p < 0.05$, ** $p < 0.01$.

243 at any of the tested concentrations (0.1–10 μ M) ($p > 0.05$)
244 (Figure 3E).

245 **Gastrointestinal Stability Assays Revealed a Stable**
246 **and Bioactive TFF3 Metabolite.** TFF3 is often considered
247 metabolically stable due to its rigid disulfide-rich structure and
248 function in the gut.³ However, no systematic gut stability
249 studies have been carried out and some reports indicate that
250 TFF3 is not fully resistant to proteases. For example, only 15%
251 of intravenously injected iodine-labeled TFF3 homodimer in

rats was recovered from urine after 24 h.²⁶ TFF3 homodimer
252 was also degraded in the terminal parts of the large intestine²⁷
253 and truncated at the C-terminal Phe⁵⁹ in human saliva.²⁸ It was
254 thus important to characterize TFF3's gastrointestinal stability
255 in more detail, particularly considering that studies often rely
256 on the use of sodium dodecyl sulfate (SDS) gels and
257 antibodies to identify and characterize TFF3, where
258 truncations can easily be missed.^{48,49,66}
259

260 We exposed TFF3(C⁵⁷Acm) and TFF3 homodimer to
261 simulated gastric fluid (SGF, containing pepsin, pH 1.3) and
262 simulated intestinal fluid (SIF, containing pancreatic enzymes,
263 pH 6.8), and monitored the mixture over 24 h by analytical
264 RP-HPLC and MS. The N- and C-termini of TFF3 and its
265 homodimer were readily truncated in both SGF and SIF
266 (Figure 4A,B). In SGF, TFF3 was cleaved at Leu⁶/Ser⁷
267 followed by cleavage at Glu⁵⁴/Ala⁵⁵ ($t_{1/2} < 5$ min). In SIF,
268 TFF3 was cleaved first at Thr⁵⁸/Phe⁵⁹ followed by cleavage at
269 Leu⁶/Ser⁷, Glu⁵⁶/Cys⁵⁷, and Ala⁵⁵/Glu⁵⁶ ($t_{1/2} < 5$ min). TFF3
270 homodimer, in both SGF ($t_{1/2} \sim 40$ min) and SIF ($t_{1/2} < 5$
271 min), was first broken down to monomeric TFF3 through
272 simultaneous cleavage at Leu⁶ and Glu⁵⁴ or Ala⁵⁵, eventually
273 leading to the same metabolites as TFF3 (Figure 4B).
274 Importantly, we identified two metabolites (TFF3₇₋₅₄ in SGF,
275 and TFF3₇₋₅₅ in SIF) that remained stable even after 24 h
276 (Figure 4B).

277 In certain physiological environments, disulfide bonds are
278 prone to scrambling or reductive cleavage, thereby affecting
279 peptide integrity.⁶⁷ Thus, we also evaluated the stability of the
280 disulfide bonds of TFF3 in the presence of 10 equivalents of
281 reduced glutathione (GSH) at pH 7 by time-course analytical
282 RP-HPLC. No disulfide bond reduction or scrambling was
283 observed for TFF3 or its homodimer (Figure S4) under these
284 conditions. While this was expected for the relatively buried
285 disulfide bonds within the trefoil domain (TFF3₁₀₋₅₀), it
286 highlights that also the disulfide bond outside of the trefoil
287 domain is well protected.

288 We then synthesized the trefoil domain (TFF3₁₀₋₅₀, single-
289 chain assembly *via* Fmoc-SPPS) to investigate its gut stability.
290 We acetylated the N-terminus (Gln¹⁰) of the trefoil domain to
291 prevent the formation of pyroglutamic acid. TFF3₁₀₋₅₀ was
292 stable in SGF for 24 h but exhibited low stability in SIF ($t_{1/2} <$
293 30 min) (Figure 4C). We incubated TFF3₁₀₋₅₀ with trypsin to
294 identify some of the cleavage sites and observed cleavages at
295 Lys¹⁶, Arg¹⁸, and Arg⁴¹ and fragments Glu³⁰-Arg³⁴ and Ile⁴²-
296 Lys⁵⁰ linked by a disulfide bond. A comparison of the NMR
297 secondary α chemical shifts of TFF3₁₀₋₅₀ with those of full-
298 length TFF3 (BMRB: 5771) indicated that removal of the C-
299 and N-terminal tails outside the trefoil domain did not change
300 TFF3's overall domain structure (Figure 4D).

301 We also synthesized TFF3₇₋₅₄ (single-chain assembly *via*
302 Fmoc-SPPS) to confirm the initial stability results and to
303 elucidate whether the residues outside the trefoil domain
304 (S⁷AN⁹, P⁵¹LQE⁵⁴) were responsible for its greater stability.
305 TFF3₇₋₅₄ was indeed stable in SGF and SIF with a half-life over
306 24 h (Figure 4C); $\sim 25\%$ degradation was observed in SIF
307 within 24 h and MS analysis identified that cleavage mainly
308 occurred near the C-terminus (Leu⁴⁶/Gln⁴⁷ and Gln⁴⁷/Glu⁴⁸).
309 Secondary α chemical shifts of TFF3₇₋₅₄ confirmed that it
310 had the same overall fold as full-length TFF3 (Figure 4D).
311 TFF3₇₋₅₄ was also active in the anti-apoptosis assay, equivalent
312 to TFF3 and TFF3 homodimer (Figure 4E). Taken together,
313 these results suggest that the N- and C-terminal extended
314 domain residues in TFF3₇₋₅₄ provide some steric protection
315 against intestinal proteases and that the pharmacophore sits
316 within the trefoil domain.

317 ■ DISCUSSION

318 Reliable synthetic access to TFF3 and its homodimer has been
319 a long-standing challenge due to its length, difficult sequence
320 segments, disulfide-rich character, and the presence of a
321 seventh unpaired cysteine residue (Cys⁵⁷) that enables homo-

or heterodimer formation.^{1,30} Here, we achieved the chemical
synthesis of the monomers TFF3(C⁵⁷Acm) and TFF3, and the
TFF3 homodimer (Figure 1). TFF3(C⁵⁷Acm) is a valuable
TFF3 analogue that cannot dimerize under physiological
conditions, thereby enabling a more controlled study of the
effects of monomeric vs homodimeric TFF3. The synthesis
was achieved *via* a combination of Fmoc-SPPS and two-
fragment NCL followed by an efficient oxidative folding step
using well-defined conditions (Figure 1). Compared to other
approaches (i.e., recombinant expression), our strategy has the
advantage of providing full control over site-specific chemical
modifications, being compatible with combinatorial ap-
proaches and facilitating the incorporation of unnatural
amino acids, bioconjugations handles, and reporter tags. This
represents therefore an important new milestone for TFF3
research, since it considerably expands ligand design options,
important for molecular probe development, structure-activity
relationship (SAR) studies, and therapeutic lead development.

TFF3's function has been associated with high metabolic
stability to regulate gastrointestinal protection and repair,
colorectal cancer development, and neuronal protection in the
CNS.^{1,3,30} However, its mechanism of action and target
receptors remain speculative and have not been independently
validated^{1,30} and also the gastrointestinal stability has not been
systematically investigated with some studies indicating that
they are degraded.^{26,28} The presumed high gastrointestinal
stability of TFF3⁶⁸⁻⁷⁰ would be an attractive feature from a
peptide drug development point of view, since it could enable
oral administration of TFF3-like drug candidates for the
treatment of gastrointestinal disorders. With milligram
quantities of TFF3 analogues at hand, we therefore
investigated some of these aspects further to provide novel
insights into TFF3's metabolic stability and mechanisms of
action.

TFF3 and its homodimer were rapidly enzymatically
truncated at both termini in the gastric (TFF3 $t_{1/2} < 5$ min;
TFF3 homodimer $t_{1/2} \sim 40$ min) as well as in the intestinal
($t_{1/2} < 5$ min) environment (Figure 4A), revealing a gut-stable
metabolite (TFF3₇₋₅₄) (Figure 4D). The slightly shorter trefoil
domain (TFF3₁₀₋₅₀) degraded in the intestinal environment
($t_{1/2} < 30$ min) (Figure 4C), highlighting that the residues
S⁷AN⁹ and P⁵¹LQE⁵⁴ outside the trefoil domain are important
for the protection against gastrointestinal degradation. The
metabolite TFF3₇₋₅₄ retained its overall three-dimensional
structure, including its three loops and secondary motifs
(Figure 4D), and displayed similar antiapoptotic activity as
TFF3, suggesting that TFF3's pharmacophore sits within the
trefoil domain. TFF3 homodimer has been reported to be
more potent than TFF3 in promoting cell motility,^{31,32} but
considering the rapid degradation of the homodimer, it is
remains questionable if it holds a major functional role in the
gastrointestinal environment. This aligns with TFF3 being
identified predominantly as a heterodimer (TFF3-FCGBP) in
the colon, followed by the monomeric form, and only a small
portion of TFF3 observed as a homodimer.²⁹ None of the
metabolites have so far been reported, which is not surprising
considering that the methods to identify and characterize
TFF3 (i.e., SDS gels and antibodies) can easily miss terminal
truncations.^{48,49} The formation of heterodimers²⁹ and TFF3
binding to mucins might furthermore protect against
degradation.⁷¹

TFF3, TFF3 homodimer, and TFF3₇₋₅₄ all reduced
apoptosis of SH-SY5Y, a human neuroblastoma cell line 384

385 (Figure 1), aligning well with reported antiapoptotic activity,
386 including cerebral ischemia.^{22,33,72,73} These antiapoptotic
387 effects support TFF3's (neuro)protective role,^{1,33,72,73} as well
388 as its association as a tumor growth promoter in different
389 cancers.^{8,74,75} TFF3 and its homodimer did not display any
390 cytotoxic or hemolytic effects, an important aspect for future
391 therapeutic development of TFF3.

392 TFF3's interaction with CXCR4, a member of the GPCR
393 family,⁵⁸ was proposed to mediate cell migration *via* an ERK1/
394 2-independent signaling pathway.³⁹ This interaction was
395 established in a human conjunctival epithelial cell line
396 expressing CXCR4, where blockage of CXCR4 impaired
397 TFF3-mediated cell migration.³⁹ While this suggests that
398 CXCR4 is involved in the mechanism of action of TFF3, it did
399 not provide evidence of direct TFF3-CXCR4 interaction. To
400 validate this interaction, we tested TFF3 and TFF3
401 homodimer in a well-established CXCR4 signaling
402 assay,^{61–63} demonstrating that they neither activated nor
403 inhibited CXCR4 up to a concentration of 10 μM (Figure 3D).
404 These results correspond with another study that failed to co-
405 localize TFF3 and CXCR4.³⁸

406 The second putative TFF3 receptor that we investigated was
407 LINGO2, which has recently been implicated with TFF3 in
408 promoting protection against colitis *in vivo*.³⁸ Neither TFF3
409 nor TFF3 homodimer displayed any effect on LINGO2
410 dimerization, which was assessed by BRET (Figure 3E).⁵⁹ Due
411 to the limited availability of functional LINGO2 bioassays, we
412 cannot fully exclude that TFF3 does not signal through
413 LINGO2 and we can only state that TFF3 does not interfere
414 with dimerization.

415 ■ CONCLUSIONS

416 We have developed reliable synthetic strategies to produce
417 TFF3 and analogues, which will markedly facilitate mechanistic
418 and SAR studies as well as therapeutic development. We
419 revealed a gut-stable TFF3 metabolite (TFF3_{7–54}) that retained
420 its bioactivity and demonstrated that TFF3, TFF3 homodimer,
421 and the trefoil domain (TFF3_{10–50}) are readily degraded in the
422 gastrointestinal environment. We were not able to pharmaco-
423 logically confirm a TFF3 signaling or interaction with CXCR4
424 or LINGO2. The chemical synthesis of TFF3 and its
425 homodimer as well as the discovery of the truncated bioactive
426 TFF3 metabolite are important new developments for the field
427 that provide new perspectives and opportunities for the design
428 and development of advanced molecular probes and TFF3
429 analogues facilitating both fundamental research as well as
430 therapeutic development.

431 ■ EXPERIMENTAL SECTION

432 **Materials.** Fmoc-amino acids and Fmoc-Phe-Wang Tenta Gel
433 resin (loading 0.7 mmol/g) were purchased from Iris Biotech GmbH
434 (Marktredwitz, Germany). Rink amide Protide resin (loading 0.19
435 mmol/g) and Oxyma Pure (ethyl cyanohydroxyiminoacetate) were
436 obtained from CEM (Charlotte, NC). 2-Chlorotriptyl chloride resin
437 (loading 2.0 mmol/g) was from Chem-Impex (Wood Dale). Pepsin
438 from porcine gastric mucosa (3500–4500 units/mg solid), hydrazine
439 hydrate and recombinant EGF (epidermal growth factor), and *N,N'*-
440 diisopropylcarbodiimide (DIC) were from Sigma-Aldrich (Sydney,
441 Australia). *N,N*-Dimethylformamide (DMF), pancreatin from porcine
442 pancreas, trifluoroacetic acid (TFA), and diethyl ether were obtained
443 from Chem-Supply (Gillman, Australia). Trypsin-EDTA 0.25%,
444 Dulbecco's modified Eagle's medium (DMEM), and L-glutamine
445 were from Invitrogen (Mulgrave, Australia). Fetal bovine serum
446 (FBS) was from Scientifix (South Yarra, Australia). IncuCyte caspase-

3/7 green apoptosis reagent was purchased from Essenbioscience 447
(Newark Close, U.K.). HEK-293 (ATCC CRL-1573) human 448
embryonic kidney and SH-SY5Y cells were obtained from American 449
Type Culture Collection (ATCC). Chitin beads were purchased from 450
New England Biolabs GmbH (Frankfurt, Germany). IP-One Gq assay 451
kit from CisBio (Codolet, France). Metafectene Pro was from Biontex 452
Laboratories GmbH (Munich, Germany). pcDNA3.1 plasmid was 453
kindly provided by Dr. Evi Kostenis, Rheinische Friedrich-Wilhelms- 454
Universität, Bonn, Germany. All solvents were obtained in the highest 455
available purity and used without further purification. All other 456
chemicals were obtained from Sigma-Aldrich/Merck (Sydney, 457
Australia) in the highest available purity. Recombinant monomeric 458
and homodimeric human TFF3 produced in yeast were kindly 459
provided by Dr. Lars Thim (Novo Nordisk A/S, Denmark). Human 460
whole blood was obtained from the Australian Red Cross Blood 461
Service. 462

Ethics Statement. Human ethics approval was obtained for use of 463
human blood for hemolysis studies, from the University of 464
Queensland Medical Research Ethics Committee (approval number 465
2014000031). 466

Peptide Synthesis. Preparation of 2-Chlorotriptyl Hydrazine 467
Resin. 2-Chlorotriptyl chloride resin was swelled in 50% DMF/DCM 468
(v/v) for 30 min in a peptide synthesis vessel. The solution was 469
drained, and the resin was treated with 10% hydrazine hydrate/DMF 470
(v/v) for 30 min. After draining the solution, the resin was washed 471
with DMF. Unreacted resin was capped with 5% MeOH/DMF (v/v) 472
for 10 min and washed with DMF. The resin was directly used for the 473
next coupling step. Resin loading was determined by quantitative 474
Fmoc release. Briefly, 20% piperidine/DMF was added to a 10 mL 475
volumetric flask containing 10 mg of dry resin and mixed for 30 min. 476
A UV cuvette was filled with 100 μL of the supernatant and diluted 477
1:10 with 20% piperidine/DMF. The absorbance of the dibenzo- 478
fulvene-piperidine adduct was measured using a UV spectrometer at 479
301 nm. The resin loading (mmol/g) was then calculated using the 480
following formula: $A/(e \times d \times m) \times 106$, where *A* is the absorbance, *e* 481
is the extinction coefficient of dibenzofulvene adduct, *m* is the mass of 482
resin (mg), and *d* is the dilution factor. 483

Solid-Phase Peptide Synthesis. NCL precursor peptide fragments 484
of TFF3 (Cys⁵⁷(Acm) and free Cys⁵⁷ forms) were synthesized on a 485
Liberty Prime automatic synthesizer (CEM, Charlotte, NC) *via* 486
Fmoc-SPPS on a 0.1 mmol scale. C-terminal fragment was 487
synthesized using Fmoc-Phe-Wang (TFF3_{36–59}) and the hydrazide 488
fragment (TFF3_{1–35}-NHNH₂) on a freshly prepared 2-chlorotriptyl 489
hydrazide resin. TFF3_{10–50} and TFF3_{7–54} were synthesized on a Rink 490
amide protide resin. Amino acid side chains were protected as follows: 491
Arg(2,2,4,6,7-pentamethyl-dihydrobenzofuran-5-sulfonyl), Asn/Gln- 492
(trityl), Asp(O-3-methylpent-3-yl), Glu(*tert*-butyl ester (OtBu)), 493
Cys(trityl or acetamidomethyl), His/Lys/Trp (*tert*-butyloxycarbonyl), 494
and Ser/Thr/Tyr(*tert*-butyl (tBu)). Fmoc deprotection was per- 495
formed using 25% pyrrolidine/DMF. Couplings (5 equiv) were 496
carried out with DIC/Oxyma Pure at 105 °C. Fmoc-amino acid/ 497
DIC/Oxyma (1:2:1). Upon completion of the peptide chain, the resin 498
was washed with DCM/MeOH. Cleavage from the resin and 499
simultaneous removal of side-chain-protecting groups was achieved 500
by treatment with 90% trifluoroacetic acid (TFA)/5% triisopropylsil- 501
lane (TIPS)/5% H₂O at 25 °C for 90 min. Following cleavage, the 502
solution was evaporated under a stream of N₂ and the products 503
precipitated and were washed with cold Et₂O and lyophilized in 50% 504
acetonitrile (ACN)/0.1% TFA/H₂O. The crude products were 505
purified by preparative HPLC. 506

Native Chemical Ligation. Only fragments with purity > 90% were 507
used for the NCL. The N-terminal fragment containing the hydrazide 508
group (1.5 mM) was oxidized to an azide by dissolving the peptide in 509
0.2 M sodium phosphate buffer solution containing 6 M Gn-HCl (pH 510
3) and reacting it with NaNO₂ (10 equiv relative to the hydrazide 511
fragment) for 15 min at –15 °C. During this step, the C-terminal 512
fragment (1 mM) was dissolved in 0.2 M phosphate solution 513
containing 6 M Gn-HCl and sodium 2-mercaptoethanesulfonate 514
(MESNA; 100 equiv relative to the hydrazide fragment). The 515
solutions containing the peptide segments were combined, and the 516

517 pH was carefully adjusted to 7.5 with NaOH. The reaction was
518 monitored by analytical RP-HPLC and carried out for 24 h and
519 purified by preparative RP-HPLC. TCEP (75 mM) was added to the
520 reaction before RP-HPLC analysis and purification.

521 **Oxidative Folding.** Peptides were dissolved in a minimal amount of
522 50% ACN/0.1% TFA/H₂O and added to the oxidative buffer (0.1 M
523 NH₄HCO₃) for a final concentration of 50 μ M, and the pH was
524 adjusted to 8.5. Oxidation was monitored by analytical RP-HPLC and
525 electrospray mass spectroscopy (ESI-MS). After complete oxidation,
526 the pH was adjusted to 2 with neat TFA, filtered, and the peptide was
527 purified by preparative RP-HPLC.

528 **Dimerization.** Folded monomeric TFF3 with the Cys⁵⁷ unpro-
529 tected was dissolved in 50% ACN/0.1% TFA/H₂O to a final
530 concentration of 2.5 mM. Iodine (30 equiv) was added to accelerate
531 the dimerization. After complete oxidation (2 min), the reaction was
532 quenched with ascorbic acid and the peptide was purified by
533 preparative RP-HPLC (~60% yield).

534 **RP-HPLC and LC-MS Methods.** Peptides were purified using either
535 a preparative C₁₈ (Grace Vydac; 10 μ m, 2.2 cm ID \times 250 mm, flow
536 rate 15 mL/min) or C₅ (Phenomenex Luna; 10 μ m, 21.2 mm ID \times
537 250 mm, flow rate 15 mL/min) columns on a Waters 600 HPLC
538 system (Waters Co., Milford, MA) using gradient of solvent A (0.05%
539 TFA in water) and B (90% ACN/0.043% TFA/10% H₂O) according
540 to the peptide retention time observed by analytical RP-HPLC.
541 TFF3₁₋₃₅ was purified using the C₁₈ preparative RP-HPLC column
542 with a gradient of 10–40% B over 60 min (15% yield). TFF3₃₆₋₅₉
543 (20% yield) and reduced TFF3 (19% yield) were also purified on the
544 C₁₈ preparative column with a gradient of 20–50% B over 60 min.
545 Reduced TFF3 was washed with 10% B for 15 min before its
546 purification to remove the salts from the ligation buffer. Folded TFF3
547 was purified using the C₅ preparative RP-HPLC column with a
548 gradient of 10–40% B over 60 min. The molecular mass of the
549 fractions collected was analyzed by direct injection in an ESI-MS, and
550 those with the desired mass were further analyzed by RP-HPLC and
551 lyophilized. Peptides were analyzed by RP-HPLC using an analytical
552 C₃ (Agilent Zorbax SB-C₃, 5 μ m, 2.1 mm \times 250 mm, 300 Å) or C₁₈
553 (Phenomenex Jupiter; 5 μ m, 2.1 mm \times 250 mm, 300 Å) RP-HPLC
554 column connected to a Shimadzu LC-20AT solvent delivery system
555 equipped with an SIL-20AHT autoinjector and an SPD-20A
556 Prominence ultraviolet–visible detector. Data were recorded and
557 processed with the Shimadzu LabSolutions software (version 5.90). A
558 linear gradient from 0 to 60% solvent B in 60 min was performed
559 (solvent A 0.05% TFA in water and B 90% ACN/0.043% TFA/10%
560 H₂O), and absorbance data were collected at 214 nm to determine
561 the purity of the final product. Only peptides with purity >95% were
562 used for structural and biological analyses. The mass analysis of the
563 peptides was performed using a Q-Star Pulsar mass spectrometer
564 (SCIEX, Ontario, Canada) with a Series 1100 solvent delivery system
565 equipped with an autoinjector (Agilent Technologies, Inc., Palo Alto,
566 CA) and a Phenomenex Jupiter LC-MS C₁₈ column (90 Å, 4 μ m, 2
567 mm \times 250 mm). Linear gradients of 0.1% aqueous formic acid
568 (solvent A) and 90% ACN/0.1% formic acid (solvent B) were
569 employed at a flow rate of 250 μ L/min, and the column was
570 maintained at 45 °C. The instrument was scanned in the *m/z* range of
571 500–1800 Da. Data acquisition and processing were carried out using
572 Analyst software v1.1 (SCIEX, Canada).

573 **Co-elution RP-HPLC Study of TFF3 Homodimer.** Synthetic and
574 recombinant homodimeric TFF3 were co-injected at a 2:1
575 (synthetic:recombinant) ratio and subjected to analytical RP-HPLC
576 analysis using a 1% solvent B/min gradient on a C₃-RP-HPLC
577 column (Agilent Zorbax SB-C₃, 5 μ m, 2.0 mm \times 250 mm, 300 Å).

578 **In Vitro Stability Assay.** Simulated gastric fluid (SGF) was
579 prepared by dissolving 20 mg of NaCl and 8 mg of pepsin in 70
580 μ L of concentrated HCl (32%), and the volume was diluted to 10 mL
581 with Milli-Q water (pH 1.3).^{76,77} Simulated intestinal fluid (SIF) was
582 prepared by dissolving 68 mg of KH₂PO₄ in 500 μ L of Milli-Q water
583 followed by the addition of 800 μ L of 0.2 M NaOH and 100 mg of
584 porcine pancreatin, and the volume was adjusted to 10 mL with Milli-
585 Q water (pH 6.8).^{76,77} Peptide stock solution (1 mM; 15 μ L) was
586 added to SGF (285 μ L) or SIF (285 μ L) and incubated at 37 °C.

587 Samples (30 μ L) from SGF and SIF were taken at 0, 5, 15, and 30
588 min and 1, 2, 4, 8, and 24 h timepoints and subsequently quenched
589 with 30 μ L of 0.2 M Na₂CO₃ (SGF) or 30 μ L of 5% aqueous TFA
590 (SIF). The samples were analyzed by analytical RP-HPLC (30 μ L)
591 and/or LC-MS (20 μ L). The amount of peptide remaining was
592 determined by measuring the peak area and expressing it as a % of the
593 peak area at time 0. Peptide half-life (*t*_{1/2}) was determined from the
594 peptide degradation profiles using an exponential one-phase decay fit
595 in Prism (version 7, GraphPad, La Jolla). LC-MS analysis was
596 performed in a Q-Star Pulsar mass spectrometer (SCIEX, Ontario,
597 Canada), and the raw data spectra were processed using the peptide
598 reconstruction tool in the BioAnalyst software to identify the mass of
599 the metabolites. The stability of the disulfide bonds was assessed
600 through incubation of the peptides (10 μ M) with 10 equiv of reduced
601 glutathione (GSH; 100 μ M) in sodium phosphate (50 mM) buffer at
602 pH 7.2. Samples were taken at timepoints 0, 4, 8, and 24 h, quenched
603 by adding 10% TFA, and analyzed by analytical RP-HPLC using an
604 analytical C₃ column (Agilent Zorbax SB-C₃, 5 μ m, 2.1 mm \times 250
605 mm, 300 Å).

606 **Circular Dichroism.** Stock solutions of the peptides were prepared
607 in 50% ACN/H₂O at 1 mM concentration. Peptide concentrations for
608 CD analysis were 50 μ M in 10 mM sodium phosphate buffer (pH
609 7.4). CD spectra were obtained on a Jasco J-810 spectropolarimeter
610 (Easton, MD). All experiments were carried out in a 0.1 cm quartz
611 cell with 250 μ L of sample at 25 °C and examined in the far-UV
612 spectra region (185–260 nm), 20 nm/min scanning speed, 1 nm
613 bandwidth, and 0.5 nm data pitch with five scans averaged for each
614 sample. Blank subtraction was performed in the Spectra Management
615 Software followed by smoothing using the Savitzky–Golay method.
616 CD was reported as mean residue ellipticity ($[\theta]$ (mdeg·cm²·dmol⁻¹)
617 = (100 \times θ)/(*n* \times *c* \times *l*), where θ is the raw output (mdeg), *n* is the
618 number of peptide bonds, *c* is the concentration (M), and *l* is the
619 cuvette path length (cm)).

620 **Nuclear Magnetic Resonance.** NMR spectra of peptides dissolved
621 in 90% H₂O/10% D₂O (~1 mM) were recorded using a Bruker 600
622 MHz Avance III NMR spectrometer equipped with a cryogenically
623 cooled probe (cryoprobe) at 298 K. NOESY spectra was recorded
624 with a mixing time of 200 ms and TOCSY with spin lock of 80 ms.
625 Samples were internally referenced to water at 4.76 ppm. TopSpin
626 (Bruker Biospin) and CCPNMR Analysis 2.4.1 (CCPN, University of
627 Cambridge, Cambridge, U.K.) were used to process and assign the
628 spectra, respectively. NOEs in the NOESY spectrum were manually
629 picked and assigned. Secondary shifts were calculated by subtracting
630 the random coil α shift from the experimental α shifts.⁵⁷

631 **Antiapoptotic Assay.** SH-SY5Y cells were seeded (13–15 \times 10³
632 cells/well) in 96-well microplates in DMEM with 10% (v/v) fetal calf
633 serum (FCS; Gibco), 2 mM L-glutamine, and 100 units/mL
634 penicillin/streptomycin. The media was replaced with low riboflavin,
635 complete Ham's F12 medium with 10% (v/v) fetal calf serum, 2 mM
636 L-glutamine, and 100 units/mL penicillin/streptomycin before the
637 live-cell imaging. Cells were treated with the etoposide or the caspase-
638 3 inhibitor or TFF3 monomer or homodimer in the presence of
639 InCuCyte caspase-3/7 green apoptosis reagent. Data were acquired
640 using an InCuCyte ZOOM instrument with standard scan type setting
641 (4 images per well) every 2 h for 48 h.

642 **Cell Viability/Cytotoxicity Assays.** HEK-293 cells (5000 cells/
643 well), suspended in DMEM supplemented with 10% FBS, were
644 seeded into 384-well plates in a volume of 20 μ L. Monomeric and
645 homodimeric TFF3 were added to the cells for a final concentration
646 of 0.18–22.7 μ M. The cell plates were then incubated for 20 h at 37
647 °C and 5% CO₂. Tamoxifen was used as a positive control. After the
648 incubation, 5 μ L of 100 μ M resazurin diluted in PBS was added to
649 each well (final concentration ~11 μ M). The plates were then
650 incubated for 3–4 h at 37 °C and 5% CO₂. The fluorescence intensity
651 (FI) was read using the TECAN Infinite M1000 PRO with
652 excitation/emission 560/590 nm. Cytotoxicity or cell viability was
653 calculated using the following equation: cell viability (%) = (FI_{sample} –
654 FI_{negative}/FI_{untreated} – FI_{negative}) \times 100. CC₅₀ (concentration at 50% cell
655 viability) was calculated using a nonlinear regression analysis of log
656 (concentration) vs normalized cell viability.

657 **Hemolysis Analysis.** Monomeric and homodimeric TFF3 were
658 serially diluted twofold in 0.9% NaCl and seeded (25 μ L) in a 384-
659 well polypropylene plate (0.2–25 μ M final concentration). Whole
660 blood (10 mL/tube) was washed two to three times in three volumes
661 of 0.9% NaCl, with centrifugation of 500g, with reduced deceleration,
662 for 10 min between washes. The cells were counted using a Neubauer
663 hemocytometer and then diluted to 1×10^8 /mL in 0.9% NaCl. The
664 cells (25 μ L/well) were added to the plates containing TFF3. Melittin
665 was used as a positive control. The plates were sealed and then placed
666 on a plate shaker for 10 min before being incubated for 1 h at 37 °C
667 without shaking. Following incubation, the plates were centrifuged at
668 1000g for 10 min to pellet cells and debris and then 25 μ L of the
669 supernatant was transferred into a 384-well flat-bottom PS plate and
670 absorbance (Abs) was read at 405 nm using a Tecan M1000 Pro
671 monochromator plate reader. Percent hemolysis was calculated using
672 the following equation: Hemolysis (%) = $(\text{Abs}_{\text{sample}} - \text{Abs}_{\text{negative}} /$
673 $\text{Abs}_{\text{positive}} - \text{Abs}_{\text{negative}}) \times 100$. HC₁₀ and HC₅₀ (concentration at 10
674 and 50% hemolysis, respectively) were calculated using nonlinear
675 regression analysis of log (concentration) vs normalized hemolysis.

676 **Recombinant Expression and Purification of Human CXCL12.**
677 The human CXCL12 (natural CXCR4 ligand) cDNA was cloned into
678 the pTXB1 vector *via* Nde I and Sap I restriction sites. Generated
679 plasmids were amplified in *E. coli* DH5 α in Luria-Bertani (LB)
680 medium with 100 μ g/mL ampicillin and purified by the PureYield
681 plasmid miniprep system (Promega GmbH, Mannheim, Germany).
682 The correctness of the generated constructs was verified by Sanger
683 dideoxy sequencing of the entire CXCL12 sequence. CXCL12 was
684 expressed as fusion protein with a small intein domain from the
685 *Mycobacterium xenopi gyrA* gene and a chitin-binding domain (CBD)
686 in *E. coli* ER2566 in LB medium containing 100 μ g/mL ampicillin for
687 5 h at 37 °C under shaking. Notably, the initial methionine, which is
688 not present in the mature human protein, is not cleaved by *E. coli*;
689 thus, the generated protein bears an additional N-terminal
690 methionine.⁷⁸ After cell lysis, and inclusion body extraction and
691 solubilization, fusion protein was purified on chitin beads and target
692 protein was eluted with column buffer (20 mM HEPES, 500 mM
693 NaCl, 1 mM EDTA, 3 M urea, pH 8 at 4 °C) containing 0.1 M DTT
694 (dithiothreitol) and 0.2% Tween-20, according to the manufacturer's
695 protocol. The protein thioester was subsequently hydrolyzed under
696 basic conditions at pH 10 and 4 °C, and the target protein was
697 purified by preparative RP-HPLC on a Phenomenex Jupiter C₁₈
698 column (300 Å, 5 μ m, 250 mm \times 21.2 mm) using linear gradients of
699 0.1% TFA/H₂O and 0.08% TFA/ACN. The protein was restored in
700 0.1 M NaH₂PO₄, 6 M guanidine hydrochloride, pH 6.0, and refolded
701 by rapid dilution as described earlier.⁷⁹ Finally, refolded protein was
702 isolated *via* preparative RP-HPLC on a Phenomenex Jupiter C₁₈
703 column (300 Å, 5 μ m, 250 mm \times 21.2 mm) applying linear gradients
704 of 0.1% TFA/H₂O and 0.08% TFA/ACN. Identity and purity were
705 determined with ESI-/MALDI-ToF mass spectrometry (Bruker
706 Daltonik GmbH, Bremen, Germany) and analytical RP-HPLC,
707 respectively. The protein concentration was determined by photo-
708 metric measurement at 280 nm using the corresponding extinction
709 coefficient.

710 **Inositol 1 Phosphate (IP1) Assay.** COS-7 cells (fibroblast-like cells
711 from African green monkey) were transiently co-transfected with the
712 CXCR4 C-terminally fused to eYFP in pVito2 vector and the
713 untagged chimeric G protein $G\alpha_{\Delta 6q14myr}$ in pcDNA3.1 plasmid using
714 Metafectene Pro according to manufacturer's protocol. The cells were
715 cultured in DMEM with higher glucose and supplemented with 10%
716 FCS without any antibiotics at 37 °C and 5% CO₂ in 95% humidity.
717 Cisbio IP-One G_i assay kit was used according to previous description
718 with minor modifications to measure activity.⁸⁰ Briefly, a standard
719 curve was prepared in HBSS (Hanks' balanced salt solution) with 20
720 mM LiCl to determine the linear range of the assay and 10 000 cells/
721 well were cultured overnight in a 384-well flat white plate (Greiner
722 Bio-one GmbH, Frickenhausen, Germany). TFF3 and its homodimer
723 as well as CXCL12 were diluted in HBSS containing 20 mM LiCl.
724 Stimulation was carried out for 1 h in triplicate at 37 °C.
725 Subsequently, 3 μ L of IP1-d2 and 3 μ L of Ab-cryptate in lysis buffer
726 were added to the wells and incubated on a tumbler for 60 min at 25

°C. Fluorescence was then measured at 620 and 665 nm and the
HTRF (homogeneous time-resolved fluorescence) ratio (665/620
nm) was calculated. Data analysis was performed with Prism (version
7, GraphPad, La Jolla). Tested compounds were normalized to
CXCL12 wild type, with the highest HTRF ratio set to 0% and the
lowest HTRF ratio set to 100% response. For testing the agonistic
activity TFF3 monomer, TFF3 homodimer and CXCL12 were
individually used for stimulation in the concentration range of 10⁻¹²
to 10⁻⁵ M. Antagonistic activity was tested by stimulation of the cells
with CXCL12 in the concentration range of 10⁻¹² to 10⁻⁵ M after
preincubation for 5 min with 1.5-fold concentrated TFF3 or its
homodimer, respectively. The final concentration range of 10⁻¹² to
10⁻⁵ M to CXCL12 and 1 or 10 μ M to TFF3 monomer and
homodimer was achieved by adding the compounds from a threefold
concentrated stock solution.

Bioluminescence Resonance Energy Transfer (BRET) Assay.
HEK-293 cells were cultured with 10% FBS at 37 °C and 5% CO₂
in DMEM for 72–96 h. The cells were passaged to collagen-
pretreated 10 cm plates (1/200 dilution) and incubated at 37 °C and
5% CO₂ overnight. The medium was changed 1 h before transfection.
BRET assays were performed following transient transfection of the
donor protein (LINGO2-RLuc) alone or with the acceptor protein
(LINGO2-YFP) using the calcium phosphate method. The cells were
rinsed twice with sterile PBS 1 \times and incubated in fresh DMEM with
10% FBS at 37 °C and 5% CO₂ overnight 1 day after transfection.
Following 48 h of transfection, the medium was removed and the cells
were rinsed twice with PBS 1 \times and harvested with 10 mL of HBSS at
25 °C. The cell suspension was seeded in quadruplets in a 96-well
plate (~10 000 cells/well) in which different concentrations of
monomeric and homodimeric TFF3 have been loaded. After 20 min
incubation, the fluorescence was measured on a Mithras LB 940
Multimode Microplate Reader (Berthold Technologies, Germany) to
check if the peptides alone did not modify fluorescent emission of
YFP following excitation at 485 nm and reading at 530 nm. Then,
total luminescence was measured by following coelenterazine addition
(final concentration 5 μ M). BRET signal was measured in four
repeats and calculated by determining the emission ratio at 530/480
nm on cells coexpressing donor and acceptor and by subtracting the
emission background BRET signal ratio (530/480 nm) of cells
expressing only donor protein, then multiplying by 1,000 to obtain
results in millBRET units (mBU).

■ ASSOCIATED CONTENT

Supporting Information

The Supporting Information is available free of charge at
<https://pubs.acs.org/doi/10.1021/acs.jmedchem.1c00767>.

Oxidative folding of TFF3, analytical HPLC and high-
resolution MS traces of TFF3(C⁵⁷Acm) chemical
synthesis, analytical HPLC profile of TFF3, and stability
of TFF3 disulfide bonds (PDF)
Molecular formula strings (CSV)

■ AUTHOR INFORMATION

Corresponding Author

Markus Muttenthaler – Institute for Molecular Bioscience,
The University of Queensland, Brisbane, QLD 4072,
Australia; Institute of Biological Chemistry, Faculty of
Chemistry, University of Vienna, 1090 Vienna, Austria;
orcid.org/0000-0003-1996-4646; Phone: (+43) 1 4277
70515; Email: markus.muttenthaler@univie.ac.at

Authors

Nayara Braga Emidio – Institute for Molecular Bioscience,
The University of Queensland, Brisbane, QLD 4072,
Australia; orcid.org/0000-0001-7835-9636
Rajeshwari Meli – Institute of Biological Chemistry, Faculty of
Chemistry, University of Vienna, 1090 Vienna, Austria

791 Hue N. T. Tran – Institute for Molecular Bioscience, The
792 University of Queensland, Brisbane, QLD 4072, Australia;
793 orcid.org/0000-0001-5181-1899

794 Heyeon Baik – Institute of Biological Chemistry, Faculty of
795 Chemistry, University of Vienna, 1090 Vienna, Austria

796 Séverine Morisset-Lopez – Centre de Biophysique
797 Moléculaire, CNRS, Unité Propre de Recherche 4301,
798 Université d'Orléans, 45071 Orleans, France

799 Alysha G. Elliott – Institute for Molecular Bioscience, The
800 University of Queensland, Brisbane, QLD 4072, Australia;
801 orcid.org/0000-0002-2983-0484

802 Mark A. T. Blaskovich – Institute for Molecular Bioscience,
803 The University of Queensland, Brisbane, QLD 4072,
804 Australia; orcid.org/0000-0001-9447-2292

805 Sabrina Spiller – Institute of Biochemistry, Faculty of Life
806 Sciences, Leipzig University, Leipzig 04103, Germany

807 Annette G. Beck-Sickinger – Institute of Biochemistry,
808 Faculty of Life Sciences, Leipzig University, Leipzig 04103,
809 Germany; orcid.org/0000-0003-4560-8020

810 Christina I. Schroeder – Institute for Molecular Bioscience,
811 The University of Queensland, Brisbane, QLD 4072,
812 Australia; Center for Cancer Research, National Cancer
813 Institute, National Institutes of Health, Frederick, Maryland
814 21702, United States; orcid.org/0000-0002-6737-6374

815 Complete contact information is available at:

816 <https://pubs.acs.org/10.1021/acs.jmedchem.1c00767>

817 Author Contributions

818 N.B.E., C.I.S., and M.M. conceived the idea. N.B.E., M.M., and
819 C.I.S. designed and supervised the experiments. N.B.E. and
820 H.N.T.T. performed chemical synthesis and gastrointestinal
821 stability assays. N.B.E. and C.I.S. performed structural analysis.
822 N.B.E. and H.B. carried out migration, and R.M. performed
823 anti-apoptosis assays. S.M.-L. performed the BRET assay.
824 M.A.T.B. and A.G.E. carried out the cytotoxicity and hemolysis
825 assays. S.S. performed and A.G.B.-S. supervised the CXCR4
826 assays. N.B.E. analyzed the data and wrote the manuscript. All
827 authors discussed the data, provided critical feedback, and
828 commented on the manuscript. The manuscript was written
829 through contributions of all authors. All authors have given
830 approval to the final version of the manuscript.

831 Notes

832 The authors declare no competing financial interest.

833 ACKNOWLEDGMENTS

834 M.M. was supported by the European Research Council
835 (ERC) under the European Union's Horizon 2020 research
836 and innovation program (714366) and by the Australian
837 Research Council (ARC) (DE150100784, DP190101667).
838 C.I.S. was an ARC Future Fellow (FT160100055). R.M. was
839 supported by the Austrian Science Fund (FWF) and Hertha
840 Firnberg program (T948-B27). N.B.E. was supported by the
841 University of Queensland International Postgraduate Scholar-
842 ship. The authors thank Janet Reid and CO-ADD (the
843 Community for Open Antimicrobial Drug Discovery), funded
844 by the Wellcome Trust (Strategic Award 104797/Z/14/Z)
845 and the University of Queensland, for the cytotoxicity and
846 hemolysis assays. They thank Dr. Lars Thim (Novo Nordisk
847 A/S) for providing the recombinant TFF3, and Prof. Paul
848 Alewood (The University of Queensland) for his overall
849 support of this work.

850 ABBREVIATIONS

BRET, bioluminescence resonance energy transfer; CD, 851
circular dichroism; CXCL12, C-X-C motif chemokine 12; 852
CXCR4, chemokine receptor type 4; CNS, central nervous 853
system; EGFR, enhanced epidermal growth factor receptor; 854
FCGBP, Fc fragment of IgG Fc binding protein; Fmoc-SPPS, 855
9-fluorenylmethyloxycarbonyl-solid-phase peptide synthesis; 856
GSH, reduced glutathione; HEK-293, human embryonic 857
kidney 293; IBD, inflammatory bowel diseases; LINGO2, 858
leucine-rich repeat receptor and nogo-interacting protein 2; 859
MESNA, sodium 2-mercaptoethanesulfonate; NOESY, nuclear 860
Overhauser effect spectroscopy; NMR, nuclear magnetic 861
resonance; SGF, simulated gastric fluid; SIF, simulated 862
intestinal fluid; TOCSY, total correlation spectroscopy 863

864 REFERENCES

- (1) Braga Emidio, N.; Brierley, S. M.; Schroeder, C. I.; Muttenthaler, 865
M. Structure, function, and therapeutic potential of the trefoil factor 866
family in the gastrointestinal tract. *ACS Pharmacol. Transl. Sci.* **2020**, 867
3, 583–597. 868
- (2) Taupin, D.; Podolsky, D. K. Trefoil factors: Initiators of mucosal 869
healing. *Nat. Rev. Mol. Cell Biol.* **2003**, 4, 721. 870
- (3) Thim, L.; May, F. E. B. Structure of mammalian trefoil factors 871
and functional insights. *Cell. Mol. Life Sci.* **2005**, 62, 2956–2973. 872
- (4) Aihara, E.; Engevik, K. A.; Montrose, M. H. Trefoil factor 873
peptides and gastrointestinal function. *Annu. Rev. Physiol.* **2017**, 79, 874
357–380. 875
- (5) Dignass, A.; Lynch-Devaney, K.; Kindon, H.; Thim, L.; 876
Podolsky, D. K. Trefoil peptides promote epithelial migration through 877
a transforming growth factor beta-independent pathway. *J. Clin. Invest.* 878
1994, 94, 376–383. 879
- (6) Hoffmann, W.; Jagla, W.; Wiede, A. Molecular medicine of TFF- 880
peptides: from gut to brain. *Histol. Histopathol.* **2001**, 16, 319–334. 881
- (7) Schwarz, H.; Jagla, W.; Wiede, A.; Hoffmann, W. Ultrastructural 882
co-localization of TFF3-peptide and oxytocin in the neural lobe of the 883
porcine pituitary. *Cell Tissue Res.* **2001**, 305, 411–416. 884
- (8) Perry, J. K.; Kannan, N.; Grandison, P. M.; Mitchell, M. D.; 885
Lobie, P. E. Are trefoil factors oncogenic? *Trends Endocrinol. Metab.* 886
2008, 19, 74–81. 887
- (9) Jahan, R.; Shah, A.; Kisling, S. G.; Macha, M. A.; Thayer, S.; 888
Batra, S. K.; Kaur, S. Odyssey of trefoil factors in cancer: diagnostic 889
and therapeutic implications. *BBA, Biochim. Biophys. Acta, Rev. Cancer* 890
2020, No. 188362. 891
- (10) Madsen, J.; Nielsen, O.; Tormoe, I.; Thim, L.; Holmskov, U. 892
Tissue localization of human trefoil factors 1, 2, and 3. *J. Histochem.* 893
Cytochem. **2007**, 55, 505–513. 894
- (11) Mashimo, H.; Wu, D. C.; Podolsky, D. K.; Fishman, M. C. 895
Impaired defense of intestinal mucosa in mice lacking intestinal trefoil 896
factor. *Science* **1996**, 274, 262–265. 897
- (12) Farrell, J. J.; Taupin, D.; Koh, T. J.; Chen, D.; Zhao, C. M.; 898
Podolsky, D. K.; Wang, T. C. TFF2/SP-deficient mice show 899
decreased gastric proliferation, increased acid secretion, and increased 900
susceptibility to NSAID injury. *J. Clin. Invest.* **2002**, 109, 193–204. 901
- (13) Guppy, N. J.; El-Bahrawy, M. E.; Kocher, H. M.; Fritsch, K.; 902
Qureshi, Y. A.; Poulosom, R.; Jeffery, R. E.; Wright, N. A.; Otto, W. R.; 903
Alison, M. R. Trefoil factor family peptides in normal and diseased 904
human pancreas. *Pancreas* **2012**, 41, 888–896. 905
- (14) Longman, R. J.; Douthwaite, J.; Sylvester, P. A.; Poulosom, R.; 906
Corfield, A. P.; Thomas, M. G.; Wright, N. A. Coordinated 907
localisation of mucins and trefoil peptides in the ulcer associated 908
cell lineage and the gastrointestinal mucosa. *Gut* **2000**, 47, 792–800. 909
- (15) Alison, M. R.; Chinery, R.; Poulosom, R.; Ashwood, P.; 910
Longcroft, J. M.; Wright, N. A. Experimental ulceration leads to 911
sequential expression of spasmolytic polypeptide, intestinal trefoil 912
factor, epidermal growth-factor and transforming growth-factor-alpha 913
messenger-RNAs in rat stomach. *J. Pathol.* **1995**, 175, 405–414. 914

- 915 (16) Aamann, L.; Vestergaard, E. M.; Groenbaek, H. Trefoil factors
916 in inflammatory bowel disease. *World J. Gastroenterol.* **2014**, *20*,
917 3223–3230.
- 918 (17) Furuta, G. T.; Turner, J. R.; Taylor, C. T.; Hershberg, R. M.;
919 Comerford, K.; Narravula, S.; Podolsky, D. K.; Colgan, S. P. Hypoxia-
920 inducible factor 1-dependent induction of intestinal trefoil factor
921 protects barrier function during hypoxia. *J. Exp. Med.* **2001**, *193*,
922 1027–1034.
- 923 (18) Arnold, P.; Rickert, U.; Helmers, A. K.; Spreu, J.;
924 Schneppenheim, J.; Lucius, R. Trefoil factor 3 shows anti-
925 inflammatory effects on activated microglia. *Cell Tissue Res.* **2016**,
926 *365*, 3–11.
- 927 (19) Shi, H. S.; Yin, X.; Song, L.; Guo, Q. J.; Luo, X. H.
928 Neuropeptide Trefoil factor 3 improves learning and retention of
929 novel object recognition memory in mice. *Behav. Brain Res.* **2012**,
930 *227*, 265–269.
- 931 (20) Shi, H. S.; Zhu, W. L.; Liu, J. F.; Luo, Y. X.; Si, J. J.; Wang, S. J.;
932 Xue, Y. X.; Ding, Z. B.; Shi, J.; Lu, L. PI3K/Akt signaling pathway in
933 the basolateral amygdala mediates the rapid antidepressant-like effects
934 of trefoil factor 3. *Neuropsychopharmacology* **2012**, *37*, 2671–2683.
- 935 (21) Li, J. L.; Luo, Y. X.; Zhang, R. X.; Shi, H. S.; Zhu, W. L.; Shi, J.
936 Neuropeptide trefoil factor 3 reverses depressive-like behaviors by
937 activation of BDNF-ERK-CREB signaling in olfactory bulbectomized
938 rats. *Int. J. Mol. Sci.* **2015**, *16*, 28386–28400.
- 939 (22) Liu, S. Q.; Roberts, D.; Zhang, B.; Ren, Y. P.; Zhang, L. Q.; Wu,
940 Y. H. Trefoil Factor 3 as an Endocrine Neuroprotective Factor from
941 the Liver in Experimental Cerebral Ischemia/Reperfusion Injury.
942 *PLoS One* **2013**, *8*, e77732.
- 943 (23) Hoffmann, W. TFF Peptides. In *Handbook of Biologically Active*
944 *Peptides*, Second ed.; Academic Press, 2013; pp 1338–1345.
- 945 (24) Lemercinier, X.; Muskett, F. W.; Cheeseman, B.; McIntosh, P.
946 B.; Thim, L.; Carr, M. D. High-resolution solution structure of human
947 intestinal trefoil factor and functional insights from detailed structural
948 comparisons with the other members of the trefoil family of
949 mammalian cell motility factors. *Biochemistry* **2001**, *40*, 9552–9559.
- 950 (25) Taupin, D.; Podolsky, D. K. Trefoil factors: initiators of
951 mucosal healing. *Nat. Rev. Mol. Cell. Biol.* **2003**, *4*, 721–732.
- 952 (26) Poulsen, S. S.; Thulesen, J.; Hartmann, B.; Kissow, H. L.; Nexø,
953 E.; Thim, L. Injected TFF1 and TFF3 bind to TFF2-immunoreactive
954 cells in the gastrointestinal tract in rats. *Regul. Pept.* **2003**, *115*, 91–99.
- 955 (27) Kjellef, S.; Vestergaard, E. M.; Nexø, E.; Thygesen, P.; Ehoj, M.
956 S.; Jeppesen, P. B.; Thim, L.; Pedersen, N. B.; Poulsen, S. S.
957 Pharmacokinetics of trefoil peptides and their stability in gastro-
958 intestinal contents. *Peptides* **2007**, *28*, 1197–1206.
- 959 (28) Houben, T.; Harder, S.; Schlüter, H.; Kalbacher, H.; Hoffmann,
960 W. Different forms of TFF3 in the human saliva: heterodimerization
961 with IgG Fc binding protein (FCGBP). *Int. J. Mol. Sci.* **2019**, *20*, 5000.
- 962 (29) Albert, T. K.; Laubinger, W.; Müller, S.; Hanisch, F. G.;
963 Kalinski, T.; Meyer, F.; Hoffmann, W. Human intestinal TFF3 forms
964 disulfide-linked heteromers with the mucus-associated FCGBP
965 protein and is released by hydrogen sulfide. *J. Proteome Res.* **2010**,
966 *9*, 3108–3117.
- 967 (30) Braga Emidio, N.; Hoffmann, W.; Brierley, S. M.; Muttenthaler,
968 M. Trefoil factor family: unresolved questions and clinical
969 perspectives. *Trends Biochem. Sci.* **2019**, *44*, 387–390.
- 970 (31) Marchbank, T.; Westley, B. R.; May, F. E. B.; Calnan, D. P.;
971 Playford, R. J. Dimerization of human pS2 (TFF1) plays a key role in
972 its protective/healing effects. *J. Pathol.* **1998**, *185*, 153–158.
- 973 (32) Poulsen, S. S.; Kissow, H.; Hare, K.; Hartmann, B.; Thim, L.
974 Luminal and parenteral TFF2 and TFF3 dimer and monomer in two
975 models of experimental colitis in the rat. *Regul. Pept.* **2005**, *126*, 163–
976 171.
- 977 (33) Taupin, D. R.; Kinoshita, K.; Podolsky, D. K. Intestinal trefoil
978 factor confers colonic epithelial resistance to apoptosis. *Proc. Natl.*
979 *Acad. Sci. U.S.A.* **2000**, *97*, 799–804.
- 980 (34) Chen, Y. H.; Lu, Y.; De Plaen, I. G.; Wang, L. Y.; Tan, X. D.
981 Transcription factor NF- κ B signals antianoxic function of trefoil
982 factor 3 on intestinal epithelial cells. *Biochem. Biophys. Res. Commun.*
983 **2000**, *274*, 576–582.
- (35) Chinery, R.; Playford, R. J. Combined intestinal trefoil factor
and epidermal growth-factor is prophylactic against indomethacin-
induced gastric damage in the rat. *Clin. Sci.* **1995**, *88*, 401–403.
- (36) Dürer, U.; Hartig, R.; Bang, S.; Thim, L.; Hoffmann, W. TFF3
and EGF induce different migration patterns of intestinal epithelial
cells in vitro and trigger increased internalization of E-cadherin. *Cell*
Physiol. Biochem. **2007**, *20*, 329–346.
- (37) Duraj-Thatte, A. M.; Praveschotinunt, P.; Nash, T. R.; Ward, F.
R.; Joshi, N. S. Modulating bacterial and gut mucosal interactions with
engineered biofilm matrix proteins. *Sci. Rep.* **2018**, *8*, No. 3475.
- (38) Belle, N. M.; Ji, Y.; Herbine, K.; Wei, Y.; Park, J.; Zullo, K.;
Hung, L. Y.; Srivatsa, S.; Young, T.; Oniskey, T.; Pastore, C.; Nieves,
W.; Somsouk, M.; Herbert, D. R. TFF3 interacts with LINGO2 to
regulate EGFR activation for protection against colitis and gastro-
intestinal helminths. *Nat. Commun.* **2019**, *10*, No. 4408.
- (39) Dieckow, J.; Brandt, W.; Hattermann, K.; Mentlein, R.; Schob,
S.; Schulze, U.; Ackermann, P.; Sel, S.; Paulsen Friedrich, P. CXCR4
and CXCR7 mediate TFF3-induced cell migration independently
from the ERK1/2 signaling pathway. *Invest. Ophthalmol. Visual Sci.*
2016, *57*, S6–S6.
- (40) Vandembroucke, K.; Hans, W.; Van Huysse, J.; Neiryneck, S.;
Demetter, P.; Remaut, E.; Rottiers, P.; Steidler, L. Active delivery of
trefoil factors by genetically modified *Lactococcus lactis* prevents and
heals acute colitis in mice. *Gastroenterology* **2004**, *127*, 502–513.
- (41) Tran, C. P.; Cook, G. A.; Yeomans, N. D.; Thim, L.; Giraud, A.
S. Trefoil peptide TFF2 (spasmolytic polypeptide) potently
accelerates healing and reduces inflammation in a rat model of
colitis. *Gut* **1999**, *44*, 636–642.
- (42) Babyatsky, M. W.; deBeaumont, M.; Thim, L.; Podolsky, D. K.
Oral trefoil peptides protect against ethanol- and indomethacin-
induced gastric injury in rats. *Gastroenterology* **1996**, *110*, 489–497.
- (43) Mahmood, A.; Melley, L.; Fitzgerald, A. J.; Ghosh, S.; Playford,
R. J. Trial of trefoil factor 3 enemas, in combination with oral 5-
aminosalicylic acid, for the treatment of mild-to-moderate left-sided
ulcerative colitis. *Aliment. Pharmacol. Ther.* **2005**, *21*, 1357–1364.
- (44) Peterson, D. E.; Barker, N. P.; Akhmadullina, L. I.; Rodionova,
I.; Sherman, N. S.; Davidenko, I. S.; Rakovskaya, G. N.; Gotovkin, E.
A.; Shinkarev, S. A.; Kopp, M. V.; Kulikov, E. P.; Moiseyenko, V. M.;
Gertner, J. M.; Firsov, I.; Tuleneva, T.; Yarosh, A.; Woon, C. W.
Phase II, randomized, double-blind, placebo-controlled study of
recombinant human intestinal trefoil factor oral spray for prevention
of oral mucositis in patients with colorectal cancer who are receiving
fluorouracil-based chemotherapy. *J. Clin. Oncol.* **2009**, *27*, 4333–
4338.
- (45) Thim, L.; Woldike, H. F.; Nielsen, P. F.; Christensen, M.;
Lynchdevaney, K.; Podolsky, D. K. Characterization of human and rat
intestinal trefoil factor produced in yeast. *Biochemistry* **1995**, *34*,
4757–4764.
- (46) Wang, H. B.; Tong, Y. P.; Fang, M.; Ru, B. G. High-level
expression of human TFF3 in *Escherichia coli*. *Peptides* **2005**, *26*,
1213–1218.
- (47) Le, J.; Zhang, D. Y.; Zhao, Y.; Qiu, W.; Wang, P.; Sun, Y. ITF
promotes migration of intestinal epithelial cells through crosstalk
between the ERK and JAK/STAT3 pathways. *Sci. Rep.* **2016**, *6*,
No. 33014.
- (48) Barrera, G. J.; Sanchez, G.; Gonzalez, J. E. Trefoil factor 3
isolated from human breast milk downregulates cytokines (IL8 and
IL6) and promotes human beta defensin (hBD2 and hBD4)
expression in intestinal epithelial cells HT-29. *Bosnian J. Basic. Med.*
Sci. **2012**, *12*, 256–264.
- (49) Yu, K.; Jiang, S. F.; Lin, M. F.; Wu, J. B.; Lin, J. Extraction and
purification of biologically active intestinal trefoil factor from human
meconium. *Lab. Invest.* **2004**, *84*, 390–392.
- (50) Zheng, J. S.; Tang, S.; Qi, Y. K.; Wang, Z. P.; Liu, L. Chemical
synthesis of proteins using peptide hydrazides as thioester surrogates.
Nat. Protoc. **2013**, *8*, 2483–2495.
- (51) Luo, H. B.; Cao, M. Y.; Newell, K.; Afdahl, C.; Wang, J.; Wang,
W. K.; Li, Y. L. Double-peak elution profile of a monoclonal antibody
in cation exchange chromatography is caused by histidine-

- 1053 protonation-based charge variants. *J. Chromatogr. A* **2015**, *1424*, 92–
1054 101.
- 1055 (52) Cardoso, F. C.; Dekan, Z.; Smith, J. J.; Deuis, J. R.; Vetter, I.;
1056 Herzig, V.; Alewood, P. F.; King, G. F.; Lewis, R. J. Modulatory
1057 features of the novel spider toxin mu-TRTX-Df1a isolated from the
1058 venom of the spider *Davus fasciatus*. *Br. J. Pharmacol.* **2017**, *174*,
1059 2528–2544.
- 1060 (53) Wingerd, J. S.; Mozar, C. A.; Ussing, C. A.; Murali, S. S.; Chin,
1061 Y. K.; Cristofori-Armstrong, B.; Durek, T.; Gilchrist, J.; Vaughan, C.
1062 W.; Bosmans, F.; Adams, D. J.; Lewis, R. J.; Alewood, P. F.; Mobli,
1063 M.; Christie, M. J.; Rash, L. D. The tarantula toxin beta/delta-TRTX-
1064 Pre1a highlights the importance of the S1-S2 voltage-sensor region for
1065 sodium channel subtype selectivity. *Sci. Rep.* **2017**, *7*, No. 974.
- 1066 (54) Takahashi, H.; Kim, J. I.; Min, H. J.; Sato, K.; Swartz, K. J.;
1067 Shimada, I. Solution structure of hanatoxin1, a gating modifier of
1068 voltage-dependent K(+) channels: common surface features of gating
1069 modifier toxins. *J. Mol. Biol.* **2000**, *297*, 771–780.
- 1070 (55) Braga Emidio, N.; Baik, H.; Lee, D.; Sturmer, R.; Heuer, J.;
1071 Elliott, A. G.; Blaskovich, M. A. T.; Haupenthal, K.; Tegtmeyer, N.;
1072 Hoffmann, W.; Schroeder, C. I.; Muttenthaler, M. Chemical synthesis
1073 of human trefoil factor 1 (TFF1) and its homodimer provides novel
1074 insights into their mechanisms of action. *Chem. Commun.* **2020**, *56*,
1075 6420–6423.
- 1076 (56) Muskett, F. W.; May, F. E. B.; Westley, B. R.; Feeney, J.
1077 Solution structure of the disulfide-linked dimer of human intestinal
1078 trefoil factor (TFF3): the intermolecular orientation and interactions
1079 are markedly different from those of other dimeric trefoil protein.
1080 *Biochemistry* **2003**, *42*, 15139–15147.
- 1081 (57) Wishart, D. S.; Bigam, C. G.; Holm, A.; Hodges, R. S.; Sykes, B.
1082 D. 1H, 13C and 15N random coil NMR chemical shifts of the
1083 common amino acids. I. Investigations of nearest-neighbor effects. *J.*
1084 *Biomol. NMR* **1995**, *5*, 67–81.
- 1085 (58) Lefrançois, M.; Lefebvre, M. R.; Saint-Onge, G.; Boulais, P. E.;
1086 Lamothe, S.; Leduc, R.; Lavigne, P.; Heveker, N.; Escher, E. Agonists
1087 for the Chemokine Receptor CXCR4. *ACS Med. Chem. Lett.* **2011**, *2*,
1088 597–602.
- 1089 (59) Guillemain, A.; Laouarem, Y.; Cobret, L.; Stefok, D.; Chen, W.
1090 Y.; Bloch, S.; Zahaf, A.; Blot, L.; Reverchon, F.; Normand, T.;
1091 Decoville, M.; Grillon, C.; Traiffort, E.; Morisset-Lopez, S. LINGO
1092 family receptors are differentially expressed in the mouse brain and
1093 form native multimeric complexes. *FASEB J.* **2020**, *34*, 13641–13653.
- 1094 (60) Czekanska, E. M. Assessment of cell proliferation with
1095 resazurin-based fluorescent dye. In *Methods in Molecular Biology*;
1096 Humana Press, 2011; Vol. 740, pp 27–32.
- 1097 (61) Kostenis, E. Potentiation of GPCR-signaling via membrane
1098 targeting of G protein alpha subunits. *J. Recept. Signal Transduction*
1099 *Res.* **2002**, *22*, 267–281.
- 1100 (62) Berridge, M. J. Rapid accumulation of inositol trisphosphate
1101 reveals that agonists hydrolyze polyphosphoinositides instead of
1102 phosphatidylinositol. *Biochem. J.* **1983**, *212*, 849–858.
- 1103 (63) Berridge, M. J.; Dawson, R. M. C.; Downes, C. P.; Heslop, J. P.;
1104 Irvine, R. F. Changes in the levels of inositol phosphates after agonist-
1105 dependent hydrolysis of membrane phosphoinositides. *Biochem. J.*
1106 **1983**, *212*, 473–482.
- 1107 (64) Degorce, F.; Card, A.; Soh, S.; Trinquet, E.; Knapik, G. P.; Xie,
1108 B. HTRF: A technology tailored for drug discovery - a review of
1109 theoretical aspects and recent applications. *Curr. Chem. Genomics*
1110 **2009**, *3*, 22–32.
- 1111 (65) El Khamlichi, C.; Reverchon-Assadi, F.; Hervouet-Coste, N.;
1112 Blot, L.; Reiter, E.; Morisset-Lopez, S. Bioluminescence resonance
1113 energy transfer as a method to study protein-protein interactions:
1114 application to G protein coupled receptor biology. *Molecules* **2019**, *24*,
1115 537.
- 1116 (66) Qi, G. F.; Li, J. J.; Wang, S. Y.; Xin, S. S.; Du, P.; Zhang, Q. Y.;
1117 Zhao, X. Y. A chimeric peptide of intestinal trefoil factor containing
1118 cholesteryl ester transfer protein B cell epitope significantly inhibits
1119 atherosclerosis in rabbits after oral administration. *Peptides* **2011**, *32*,
1120 790–796.
- (67) Räder, A. F. B.; Weinmuller, M.; Reichart, F.; Schumacher-
Klinger, A.; Merzbach, S.; Gilon, C.; Hoffman, A.; Kessler, H. Orally
active peptides: is there a magic bullet? *Angew. Chem., Int. Ed.* **2018**,
57, 14414–14438.
- (68) Jørgensen, K. H.; Thim, L.; Jacobsen, H. E. Pancreatic
spasmolytic polypeptide (PSP): I. preparation and initial chemical
characterization of a new polypeptide from porcine pancreas. *Regul.*
Pept. **1982**, *3*, 207–219.
- (69) Playford, R. J.; Marchbank, T.; Chinery, R.; Evison, R.;
Pignatelli, M.; Boulton, R. A.; Thim, L.; Hanby, A. M. Human
spasmolytic polypeptide is a cytoprotective agent that stimulates cell-
migration. *Gastroenterology* **1995**, *108*, 108–116.
- (70) Sun, Y.; Peng, X.; Zhang, Y.; Lv, S. J.; Wu, W.; Wang, S. L.
Stability and biological activity of human intestinal trefoil factor
produced by *Pichia pastoris*. *Protein Pept. Lett.* **2008**, *15*, 255–259.
- (71) Yu, H.; He, Y.; Zhang, X.; Peng, Z.; Yang, Y.; Zhu, R.; Bai, J.;
Tian, Y.; Li, X.; Chen, W.; Fang, D.; Wang, R. The rat IgGFcγBP and
MUC2 C-terminal domains and TFF3 in two intestinal mucus layers
bind together by covalent interaction. *PLoS One* **2011**, *6*, No. e20334.
- (72) Kinoshita, K.; Taupin, D. R.; Itoh, H.; Podolsky, D. K. Distinct
pathways of cell migration and antiapoptotic response to epithelial
injury: structure-function analysis of human intestinal trefoil factor.
Mol. Cell. Biol. **2000**, *20*, 4680–4690.
- (73) Sun, Z. R.; Liu, H. M.; Yang, Z. Z.; Shao, D. B.; Zhang, W.;
Ren, Y.; Sun, B. D.; Lin, J. F.; Xu, M.; Nie, S. N. Intestinal trefoil
factor activates the PI3K/Akt signaling pathway to protect gastric
mucosal epithelium from damage. *Int. J. Oncol.* **2014**, *45*, 1123–1132.
- (74) Hanisch, C.; Sharbati, J.; Kutz-Lohroff, B.; Huber, O.;
Einspanier, R.; Sharbati, S. TFF3-dependent resistance of human
colorectal adenocarcinoma cells HT-29/B6 to apoptosis is mediated
by miR-491-5p regulation of lncRNA PRINS. *Cell Death Discovery*
2017, *3*, No. 16106.
- (75) Liu, J.; Kim, S. Y.; Shin, S.; Jung, S.-H.; Yim, S.-H.; Lee, J. Y.;
Lee, S.-H.; Chung, Y.-J. Overexpression of TFF3 is involved in
prostate carcinogenesis via blocking mitochondria-mediated apopto-
sis. *Exp. Mol. Med.* **2018**, *50*, 1–11.
- (76) Wang, J.; Yadav, V.; Smart, A. L.; Tajiri, S.; Basit, A. W. Toward
oral delivery of biopharmaceuticals: an assessment of the gastro-
intestinal stability of 17 peptide drugs. *Mol. Pharmaceutics* **2015**, *12*,
966–973.
- (77) Braga Emidio, N.; Tran, H. N. T.; Andersson, A.; Dawson, P.
E.; Albericio, F.; Vetter, I.; Muttenthaler, M. Improving the
gastrointestinal stability of linaclotide. *J. Med. Chem.* **2021**,
DOI: 10.1021/acs.jmedchem.1c00380.
- (78) Hirel, P. H.; Schmitter, J. M.; Dessen, P.; Fayat, G.; Blanquet, S.
Extent of N-terminal methionine excision from *Escherichia coli*
proteins is governed by the side-chain length of the penultimate
amino-acid. *Proc. Natl. Acad. Sci. U.S.A.* **1989**, *86*, 8247–8251.
- (79) Baumann, L.; Prokoph, S.; Gabriel, C.; Freudenberg, U.;
Werner, C.; Beck-Sickinge, A. G. A novel, biased-like SDF-1
derivative acts synergistically with starPEG-based heparin hydrogels
and improves eEPC migration in vitro. *J. Controlled Release* **2012**, *162*,
68–75.
- (80) Wanka, L.; Babilon, S.; Kaiser, A.; Mörl, K.; Beck-Sickinge, A.
G. Different mode of arrestin-3 binding at the human Y1 and Y2
receptor. *Cell. Signalling* **2018**, *50*, 58–71.